



Western Michigan University  
ScholarWorks at WMU

---

Dissertations

Graduate College

---

12-1987

## Effect of Polymerization Conversion on the Experimental Determination of Monomer Reactivity Ratios in Copolymerization

Sevim Zeynep Erhan  
*Western Michigan University*

Follow this and additional works at: <https://scholarworks.wmich.edu/dissertations>

 Part of the Chemistry Commons

---

### Recommended Citation

Erhan, Sevim Zeynep, "Effect of Polymerization Conversion on the Experimental Determination of Monomer Reactivity Ratios in Copolymerization" (1987). *Dissertations*. 3438.  
<https://scholarworks.wmich.edu/dissertations/3438>

This Dissertation-Open Access is brought to you for free and open access by the Graduate College at ScholarWorks at WMU. It has been accepted for inclusion in Dissertations by an authorized administrator of ScholarWorks at WMU. For more information, please contact [wmu-scholarworks@wmich.edu](mailto:wmu-scholarworks@wmich.edu).



**EFFECT OF POLYMERIZATION CONVERSION ON THE EXPERIMENTAL  
DETERMINATION OF MONOMER REACTIVITY  
RATIOS IN COPOLYMERIZATION**

by

**Sevim Zeynep Erhan**

**A Dissertation  
Submitted to the  
Faculty of The Graduate College  
in partial fulfillment of the  
requirements for the  
Degree of Doctor of Philosophy  
Department of Chemistry**

**Western Michigan University  
Kalamazoo, Michigan  
December 1987**

To Dr. G. G. Lowry  
and Dr. R. C. Nagler

## ACKNOWLEDGEMENTS

I wish to express my sincere appreciation to Dr. G. G. Lowry for his patience and assistance during the course of this investigation. His helpful suggestions and critical eye were invaluable and greatly appreciated.

I also wish to acknowledge Dr. J. A. Howell, who was extremely helpful and provided much advice with respect to spectroscopic experimental techniques.

I wish to express my appreciation to all the committee members who have contributed to this work, and my friend Bülent Acar for his help in mathematical problems.

I would like to thank the Chemistry Department of Western Michigan University for the financial aid and teaching experience gained from my teaching assistantship.

Finally, I want to express my gratitude to my husband for his many sacrifices and assistance in preparing this manuscript and for his support during the course of my studies.

Sevim Zeynep Erhan

EFFECT OF POLYMERIZATION CONVERSION ON THE EXPERIMENTAL  
DETERMINATION OF MONOMER REACTIVITY  
RATIOS IN COPOLYMERIZATION

Sevim Zeynep Erhan, Ph.D.

Western Michigan University, 1987

In this study the comparison of the methods used to calculate monomer reactivity ratios from experimental copolymer composition data is targeted.

For this purpose, nine samples of each of nine different concentrations of styrene-methyl methacrylate monomer mixtures were prepared. These mixtures were then polymerized for different times ranging from one to nine hours and the percent conversion to copolymer was determined.

The compositions of these copolymers were determined by their refractive index increments measured in two different solvents. Ultraviolet absorption spectroscopy was also studied as a possible method to find copolymer compositions. Though this method has been used previously, UV absorption by copolymers appears to be related to monomer sequence so that a simple application of Beer's Law is not valid.

As the best method to calculate  $r_1$  and  $r_2$  values, the Maximum Likelihood Method was taken. This method gave  $r_1=0.495$  and  $r_2=0.467$  where styrene is monomer 1. These values were then compared to the

$r_1$  and  $r_2$  values obtained from a Nonlinear Least Squares Method, Intersection Method, Fineman-Ross Method and the Kelen-Túdős Method. From this comparison it was seen that the Nonlinear Least Squares Method gave the best results. The Intersection Method gave better results than the Kelen-Túdős Method which in turn was better than the Fineman-Ross Method. Also it was observed that the calculation method of Fineman-Ross led to inconsistent monomer reactivity ratios.

This study is concluded with recommendations for further research in the area of penultimate effect in propagation, copolymers using monomers that will give a larger composition drift, and studies on the method of UV analysis of copolymer compositions taking the absorption of methyl methacrylate into consideration.

## TABLE OF CONTENTS

ACKNOWLEDGEMENTS	. . . . .	ii
LIST OF TABLES	. . . . .	v
LIST OF FIGURES	. . . . .	vi
<b>CHAPTER</b>		
<b>I. INTRODUCTION</b>	. . . . .	<b>1</b>
Theory of Free Radical Copolymerization	. . . . .	1
Copolymer Composition Analysis	. . . . .	4
Elemental and Functional Group Analysis	. . . . .	4
Spectroscopic Analysis	. . . . .	5
Ultraviolet Spectroscopy	. . . . .	6
Infrared Spectroscopy	. . . . .	8
Nuclear Magnetic Resonance Spectroscopy	. . . . .	9
Visible Spectroscopy	. . . . .	11
Differential Refractometry	. . . . .	11
Methods of Determining $r_1$ and $r_2$ Values	. . . . .	15
Direct-Curve Fitting on Polymer-Monomer Composition Plots	. . . . .	15
Intersecting Slopes Method	. . . . .	16
Fineman and Ross Method	. . . . .	16
Kelen and Tüdős Method	. . . . .	17
Quantitative Treatment of Composition Drift	. . . . .	18
Goals of Current Research	. . . . .	22
<b>II. EXPERIMENTAL</b>	. . . . .	<b>24</b>
Preparation of Low Conversion Styrene- Methylmethacrylate Copolymers	. . . . .	24
Purification of Copolymers	. . . . .	25

Table of Contents -- Continued

<b>CHAPTER</b>		
	Determination of Copolymer Composition . . . . .	26
	Method of Obtaining Refractive Index Increments . . . . .	26
	UV Absorption Spectra of Copolymers . . . . .	28
<b>III. RESULTS AND DISCUSSION</b>		<b>29</b>
	Results of Conversion Studies . . . . .	29
	Copolymer Composition Studies with Refractive Index Increments Measurements . . . . .	30
	Evaluation of Methods of Estimating Monomer Reactivity Ratios From Experimental Data . . . . .	32
	Maximum Likelihood Method . . . . .	32
	Methods Using Extrapolated Zero-Conversion Data . . . . .	38
	Non-Linear Least Squares . . . . .	41
	Intersection Method . . . . .	41
	Fineman and Ross Method . . . . .	48
	Kelen and Túdős Method . . . . .	52
	Effect of Composition Drift With Conversion . . . . .	52
	Comparison of Methods and Discussion . . . . .	54
	Analysis of Ultraviolet Absorption Spectra of Styrene- Methyl Methacrylate Copolymer . . . . .	61
	Conclusions . . . . .	68
	Recommendations . . . . .	69
<b>APPENDICES</b>		<b>70</b>
	A. Experimental Data for Copolymerization of Styrene With Methyl Methacrylate . . . . .	71
	B. Calculated Values of Composition and Conversion for Copolymerization of Styrene With Methyl Methacrylate . . . . .	82
<b>REFERENCES</b>		<b>94</b>



LIST OF TABLES

1. Copolymer Composition Data Using Weighted Nonlinear Least Squares . . . . .	41
2. Monomer Reactivity Ratios and Uncertainties at Each Intersection Point . . . . .	45
3. Comparison of Methods . . . . .	55
4. Experimental Values of Styrene-Methyl Methacrylate Copolymers . . . . .	67

## LIST OF FIGURES

1.	Schematic Diagram of the Working Principle of a Brice-Phoenix Visual Differential Refractometer . . . .	13
2.	Diagram of the Cell of a Brice-Phoenix Visual Differential Refractometer . . . . .	13
3.	Rate of Copolymerization of Styrene and Methyl Methacrylate, in mole percent per hour, at $60.0 \pm 0.1^\circ\text{C}$ . Horizontal bars Represent Standard Error of Estimate . . . . .	31
4.	Contours Representing Surface of Residuals - Squared for Nonlinear Least Squares Fitting of Weighted Styrene-Methyl Methacrylate Copolymer Data. Points Represent Different Methods of Evaluation, Maximum Likelihood ( $\Delta$ ), Nonlinear Least Squares (O), Intersection ( $\square$ ), Kelen-Túdős ( $\diamond$ ), Fineman-Ross ( $\nabla$ ) . .	37
5.	Mole Fraction of Styrene in Copolymer Mixture ( $F_1$ ) versus Percent Mole Conversion. Circles Represent Actual Data Points, Solid Lines are Calculated Results Assuming $r_1=0.495$ and $r_2=0.467$ . . .	39
6.	Illustration of the Application of the Intersection Method to the Data of Table 1. The Values on the Graph are Approximate Monomer Compositions, Actual Compositions are Given in Table 1 . . . . .	42
7.	a: Fineman-Ross Method Using Equation 1.19, Styrene as Monomer 1 . . . . .	49
	b: Fineman-Ross Method Using Equation 1.19, Methyl Methacrylate as Monomer 1 . . . . .	49
8.	a: Fineman-Ross Method Using Equation 1.20, Styrene as Monomer 1 . . . . .	51
	b: Fineman-Ross Method Using Equation 1.20, Methyl Methacrylate as Monomer 1 . . . . .	51
9.	a: Kelen-Túdős Method, Styrene as Monomer 1 . . . . .	53
	b: Kelen-Túdős Method, Methyl Methacrylate as Monomer 1	53
10.	Instantaneous Composition of Copolymer, $F_1$ as a Function of Monomer Composition $f_1$ for the Values of Reactivity Ratios, $r_1$ and $r_2$ , 0.495 and 0.467. Circles	

List of Figures -- Continued

	Represent Copolymer Composition Extrapolated to Zero Conversion, Solid Line is Calculated Value . . . . .	56
11.	Analysis of Residuals from Nonlinear Least Squares Fitting. Lines Represent 95% Confidence Limits . . . . .	60
12.	UV Absorption of Styrene-Methyl Methacrylate Copolymer. Solid Line Represents Non-Linear Least Squares Fitted Curves Assuming Three Chromophores of Styrene Units. Dashed Line Represents Simple Beer's Law Curve . . . . .	63
13.	Overlapped Ultraviolet Absorption Spectrum of the Various Monomer Feed Compositions of Styrene-Methyl Methacrylate Copolymers all Containing 1.0mg/mL of Styrene . . . . .	64
14.	A Theoretical Plot of Triad Compositions as a Function of Monomer Compositions when $r_1=0.495$ and $r_2=0.467$ . . . . .	66

## CHAPTER I

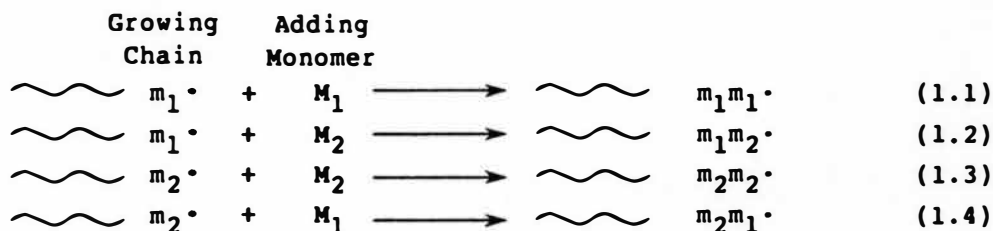
### INTRODUCTION

#### Theory of Free Radical Copolymerization

In free radical copolymerization as in ordinary free radical homopolymerization, the simple mechanistic chain reactions which lead to the formation of a polymer molecule consist of three steps: initiation, propagation, and termination. The chemical composition of high molecular weight copolymers is dependent as a first approximation only on the propagation of the chain reaction.

If one of the monomers in a copolymer is designated  $M_1$  and the other  $M_2$ , it can be shown that if the addition of these monomers of the growing radical were dependent on the makeup of the entire polymer radical, then an infinite number of different reaction rates would occur since the process would depend on both chain length and detailed composition. It was postulated as early as 1936 by Dostal<sup>1</sup> that the kinetic behavior of the chain radical was dependent only on the terminal group (the monomer unit last added to the growing chain) and that the kinetic behavior was independent of the length or over-all composition of the polymer chain.

Under these conditions the composition of the copolymer chain is determined by the following four propagation reactions:



The rates of these reactions are written as

$$-\frac{d[M_1]}{dt} = k_{11} [m_1^\cdot] [M_1] \quad (1.5)$$

$$-\frac{d[M_2]}{dt} = k_{12} [m_1^\cdot] [M_2] \quad (1.6)$$

$$-\frac{d[M_2]}{dt} = k_{22} [m_2^\cdot] [M_2] \quad (1.7)$$

$$-\frac{d[M_1]}{dt} = k_{21} [m_2^\cdot] [M_1] \quad (1.8)$$

Dostal was able to write correct mathematical expressions for the rate of copolymerization and the composition of a copolymer in terms of these rates, but since four unknown rate constants were involved he could not devise any experimental tests for his conclusions.

Wall in 1941<sup>2</sup> showed that the chemical composition of copolymers was dependent only on the relative reactivities of the two monomers to the two radicals. He expressed these relative reactivities in the form of ratios  $r_1$  and  $r_2$ , called "monomer reactivity ratios," which he defined as follows:

$$r_1 = \frac{k_{11}}{k_{12}} \quad \text{and} \quad r_2 = \frac{k_{22}}{k_{21}}$$

Mayo and Lewis<sup>3</sup> in a classic work undertook a systematic study of copolymerization and arrived at the following rate expressions for the consumption of monomers  $M_1$  and  $M_2$ , considering only the propagation reactions:

$$-\frac{d[M_1]}{dt} = k_{11} [m_1^\cdot] [M_1] + k_{21} [m_2^\cdot] [M_1] \quad (1.9)$$

$$-\frac{d[M_2]}{dt} = k_{12} [m_1^\cdot] [M_2] + k_{22} [m_2^\cdot] [M_2] \quad (1.10)$$

In the steady state of copolymerization, concentrations of different types of free radicals must be maintained constant. Therefore,  $k_{12} [m_1 \cdot] [M_2] = k_{21} [m_2 \cdot] [M_1]$ .

This means that in the steady state the rate at which  $[m_1 \cdot]$  is destroyed is equal to the rate at which  $[m_2 \cdot]$  is destroyed. It is then possible to solve for the concentration of one of the radicals in the steady state in terms of the other. Mayo and Lewis applied this steady state assumption to the ratio of the rates of disappearance of the two monomers and arrived at the following relation:

$$\frac{d[M_1]}{d[M_2]} = \left( \frac{[M_1]}{[M_2]} \right) \frac{\left( \frac{k_{11}}{k_{12}} \right) [M_1] + [M_2]}{\left( \frac{k_{22}}{k_{21}} \right) [M_2] + [M_1]} \quad (1.11)$$

Using the definition of monomer reactivity ratios defined by Wall, this can be simplified to

$$\frac{d[M_1]}{d[M_2]} = \left( \frac{[M_1]}{[M_2]} \right) \frac{r_1 [M_1] + [M_2]}{r_2 [M_2] + [M_1]} \quad (1.12)$$

It is evident that the ratio of the rates of consumption of the two monomers is also the ratio of molar concentrations of structural units derived from the two monomers in the copolymer. Defining the instantaneous concentration of monomer  $M_1$  in the copolymer as " $m_1$ " and the concentration of monomer  $M_2$  in the copolymer as " $m_2$ " then;

$$\frac{m_1}{m_2} = \left( \frac{[M_1]}{[M_2]} \right) \frac{r_1 [M_1] + [M_2]}{r_2 [M_2] + [M_1]} \quad (1.13)$$

This equation is known as the "Copolymer Composition Equation". This same equation was derived independently by Alfrey and Goldfinger<sup>4</sup> at approximately the same time using the same reasoning.

The copolymer composition equation has been used to predict the average composition of the polymer formed at any instant in the polymerization when the relative concentrations of monomers are known and the values of the monomer reactivity ratios are either known or assumed. It has also been used to calculate the values of the monomer reactivity ratios,  $r_1$  and  $r_2$ , from experimental data including the known relative concentrations of monomers and the composition of the copolymer formed. The experimental technique that is normally used consists of preparing a series of the copolymers for various  $M_1$  and  $M_2$  monomer concentrations and analyzing the resulting copolymers for the concentrations of " $m_1$ " and " $m_2$ " they contain. The conversion of the monomer to copolymer in this series must be kept low because equation (1.13) is valid only for instantaneous copolymerization, and the assumption is made that low conversion copolymerization approximates instantaneous copolymerization.

### Copolymer Composition Analysis

#### Elemental and Functional Group Analysis

The average copolymer composition can be determined by a variety of techniques including elemental and other chemical analysis. Elemental analysis is a popular method and copolymer

compositions obtained from this technique are often used to calibrate or compare with results from other techniques<sup>3</sup>. However, uncertainty as to the completeness of combustion during elemental analysis leads to uncertainty in the final results. This can be minimized by submitting samples of the  $M_1$  &  $M_2$  homopolymers to the analyst along with the copolymer samples. Automatic commercial analyzers exist which determine the carbon and hydrogen content of copolymers by combustion of the samples. Oxygen content is usually determined by difference. Also in organic compounds nitrogen is determined by Kjeldahl and Dumas methods, oxygen by neutron activation and halogens by sodium fusion.

Copolymers can also be analyzed chemically for the existence of particular functional groups. However, problems can arise due to the low solubility of copolymers or inaccessibility of functional groups<sup>5</sup>. Unique chemical procedures which are very accurate have been developed for some specific copolymers.

### Spectroscopic Analysis

When a beam of electromagnetic radiation is transmitted through a copolymer sample it may, depending on the wavelength,  $\lambda$ , be partially absorbed. Absorption processes are generally associated with some form of transition of the molecule or portion of the molecule between two energy states. The difference in energy,  $\Delta E$ , between the two energy states is a function of the wavelength,  $\Delta E = h \cdot c / \lambda$ , where  $h$  is Planck's constant and  $c$  is speed of light in vacuum.



Copolymers, as well as all other molecules, exhibit various absorption mechanisms, each characterized by a different  $\Delta E$ , and thus absorption may be observed at several different wavelengths or wavelength regions. Four regions of the electromagnetic spectrum have been traditionally used to probe copolymers and molecules in general: the ultraviolet, visible, infrared and radio-frequency regions.

### Ultraviolet Spectroscopy

The absorption of UV radiation is associated with the excitation of electrons from a ground state to a higher energy state. Specific groups or chromophores (such as carbonyl or aromatic groups) generally absorb UV radiation at specific wavelengths and have nearly the same molar absorptivity in many different molecules.

The determination of copolymer composition by UV spectroscopy would seem to be a simple matter, providing one monomer contains a UV absorbing chromophore and the other does not. Since styrene absorbs strongly in the UV, the determination of the styrene content in copolymers has been a popular method of analysis<sup>6-14</sup>.

In the use of UV spectroscopy to determine copolymer composition it is assumed that Beer's Law is valid, or a linear relationship exists between the observed absorption,  $A$ , and the

$$A = \epsilon_{\lambda} \cdot b \cdot c \quad (1.14)$$

concentration of the UV absorbing chromophore,  $c$ , where  $\epsilon_{\lambda}$  is the absorptivity and  $b$  is the path length of the cell.

Unfortunately the UV analysis of poly (styrene-methylmethacrylate) copolymer [poly (sty-co-mma)] has indicated that Beer's Law, eq. (1.14), does not seem to hold<sup>7-13</sup>. The observed hypochromism of poly (sty-co-mma) solutions has been assumed to be due to variations in microstructure or conformational changes in solution. O'Driscoll et al.<sup>8</sup> rationalized the ideal absorption behavior in terms of styrene dyads, while Stutzel et al.<sup>12</sup> proposed a model based on styrene triads. Gall and Russo<sup>10,11</sup> observed hypochromic effects over a specific copolymer composition range which varied with the solvent used, which suggested changes in conformation of the macromolecules in solution.

In spite of the evidence outlined above, UV spectroscopy has been used to analyze poly (sty-co-mma) assuming Beer's Law was applicable<sup>8,15,16</sup>.

Recently Garcia-Rubio<sup>17</sup> has critically assessed the UV literature data on a variety of styrene copolymers and suggested that eq. (1.14) is not valid since the phenyl ring of styrene is not the only UV absorbing chromophore. The following empirical relationship was derived:

$$\epsilon_c(\lambda) = \epsilon_{ps}(\lambda) \cdot P_{1w} + \epsilon_i(\lambda) \cdot (1-P_{1w}) \quad (1.15)$$

In equation (1.15),  $\epsilon_c(\lambda)$  is the copolymer absorptivity at wavelength  $\lambda$ ,  $\epsilon_{ps}(\lambda)$  is polystyrene absorptivity,  $P_{1w}$  is weight fraction of styrene in the copolymer,  $\epsilon_i(\lambda)$  is the comonomer absorptivity.

In conclusion, UV spectral analysis and Beer's Law can be applied to copolymers providing all the chromophores can be identified, although identification of all chromophores is a difficult problem. It may be possible to obtain reliable copolymer composition data from UV provided the data are treated properly.

### Infrared Spectroscopy

Infrared spectroscopy is one of the techniques used to identify polymers and copolymers. IR spectroscopy, or vibrational spectroscopy involves the variation of intermolecular distances, or molecular vibration. As an example, in a heteronuclear diatomic molecule, with only one vibrational degree of freedom, there is a fundamental frequency at which the bond stretches. The stretching or oscillating of the diatomic molecule results in an oscillating electric dipole which will interact with the oscillating electric field of light, if this light has the proper infrared frequency. Interaction results in the absorption of the IR radiation and the diatomic molecule undergoes a transition to a higher vibrational energy level. More detailed explanations can be found in Colthup et al.<sup>18</sup>.

In more complex molecules containing  $N$  atoms, there will be  $3N-6$  or  $3N-5$  (if linear molecule) fundamental vibrations, thus it would appear polymer spectra would be extremely complex. Fortunately,  $\mu \approx m$  of side group for many fundamental vibrations, and it is possible to assign IR absorption frequencies to particular vibrating bonds, functional groups or groups of atoms. The absorptions observed in the IR spectra<sup>19</sup> and Raman spectra (which

involve rotational transitions)<sup>20</sup> of complex molecules have been tabulated and assigned to various organic and inorganic functional groups.

The IR spectrum of a polymer is commonly obtained from a thin film (occasionally solutions are used). Quantitative IR investigations have been rare, since this requires knowledge of the absorptivity of the band or peak observed and of the thickness of the sample. Accurate absorptivities can be obtained from model compounds. However for solid sample the thickness of the sample is difficult to measure with good accuracy and since the film is so thin, errors in the measurement of film thickness result in very large composition errors. In the IR spectra of polymer films, an interference pattern is often seen, from which film thickness may be calculated, or at least estimated.

Another problem can arise if the polymer chains in the film are oriented, since Beer's Law assumes a random orientation<sup>21</sup>. Thus, IR-absorbing groups may be anisotropic in oriented polymers so that absorbance depends on orientation of the polymer molecule relative to the optical axis of the spectrometer.

In general, IR absorptions often are poorly resolved and in many cases it is very difficult to obtain baseline resolution, because of the overlapping peaks.

#### Nuclear Magnetic Resonance Spectroscopy

NMR is another technique for investigation of copolymer composition. It is also used to determine the steric configuration or stereochemistry of polymers.

The areas of peaks in NMR spectra are proportional to the numbers of nuclei contributing to them, regardless of their chemical binding. The fraction of a particular chemical species is the area of its resonance divided by the total area of the spectrum. Peak heights, although easily measured, are not a reliable measure of relative intensities, since peak widths, being proportional to  $T_2^{-1}$ , will in general differ for different protons. ( $T_2$  = spin-spin relaxation time.) It is much more convenient and reliable to observe the spectrum in the integral mode, if the integration is properly carried out, taking particular care to avoid differential saturation.

The  $^1\text{H}$  NMR analysis of styrene-methylmethacrylate copolymers has been an ongoing study for many years. However, Johnson *et al.*<sup>15</sup> observed significant differences between experimentally obtained copolymer composition and those calculated according to the integrated form of the copolymer composition equation, for 60°C bulk copolymerization containing 60 and 35 mole % styrene.

To explain these results these authors<sup>15</sup> suggested that the reactivity ratios were a function of conversion, with  $r_1$  and  $r_2$  both changing at conversion levels as low as 10% due to the gel effect. Dionisio and O'Driscoll<sup>16</sup> repeated the 60 mole % styrene bulk copolymerization and observed results very similar to those reported by Johnson *et al.*<sup>15</sup>.

However, Dionisio and O'Driscoll rejected the explanation that reactivity ratios were a function of conversion. Reactivity ratios, being ratios of propagation rate constants, should not be affected

by changes in the diffusional characteristics of the reaction medium, at least at conversion levels as low as 10%.

For more detail concerning the application of NMR to polymer systems, the reader is referred to Bovey<sup>22</sup>.

### Visible Spectroscopy

In the visible region, polymers and copolymers generally do not absorb, but quantitative changes in the refractive index of polymeric solutions are normally observed. Differential refractive index data generally assume the specific refractive index increment  $dn/dc$  is a constant, independent of molecular weight. However, studies by Barral et al.<sup>23</sup> and Francois et al.<sup>24</sup> have indicated the  $dn/dc$  of polystyrene to be a function of molecular weight, particularly at low molecular weight.

In their theory for light scattering in copolymer solution, Stockmayer, et al.<sup>25</sup> assume the specific refractive increment, ( $dn/dc$ ), is a colligative property of the copolymer and independent of molecular weight. The light scattering investigation of Bushuk and Benoit<sup>26</sup> and Krause<sup>27</sup> on block, graft and statistical copolymers agree with the light-scattering theory and thus justify this assumption. It is assumed in this present work, that  $dn/dc$  is independent of molecular weight.

### Differential Refractometry

Differential refractometers directly measure the difference in refractive index between a dilute solution of copolymer and its solvent with a sensitivity of about  $\pm 0.000003$ .

Figure 1 shows the working principle of a Brice-Phoenix visual differential refractometer. The monochromatic light beam coming out of the light source (A), passes through an adjustable slit (B), and goes through a sinter-fused optical glass cell (C) which contains the solution and solvent that are separated from each other by a diagonal glass partition. The glass cell is clamped so that the polished faces are perpendicular to the optic axis. The cell holder can be rotated about a vertical axis through 180°. As seen in Figure 2 when the light beam enters from the solution side and exits from the solvent side, the reading is  $d_1$ , and when the light beam enters from the solvent side and exits from the solution side, the reading is  $d_2$ . The light beam that leaves the cell, which is an image of the slit, is projected by a projector lens (D) onto the focal plane (F) of the objective of a microscope (E). The slit image can be focused by moving the microscope objective on the longitudinal axis. Values of  $d_1$  and  $d_2$  are obtained, when the movable cross-hairs in (G) are exactly in the center of the image of the slit, or the focal plane. This is done by the aid of a drum that moves the cross-hairs and is divided to 0.01mm.

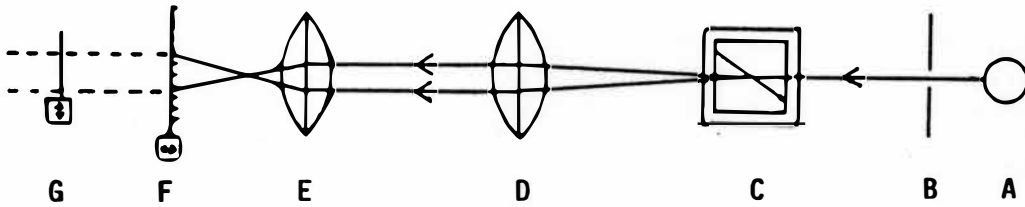


Figure 1. Schematic Diagram of the Working Principles of a Brice-Phoenix Visual Differential Refractometer.

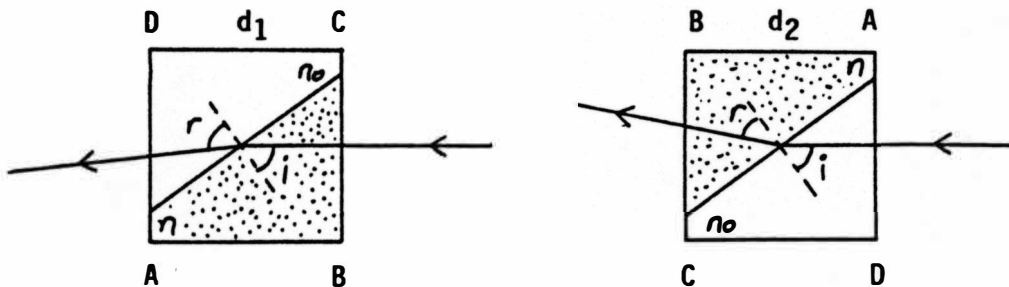


Figure 2. Diagram of the cell of a Brice-Phoenix Visual Differential Refractometer.



The refractive index difference is given by the following equation<sup>28</sup>:

$$\Delta n = k \cdot \Delta d \quad (1.16)$$

Where  $\Delta n$  is the refractive index difference between a solution and its solvent,  $k$  is the calibration constant for the selected wavelength, and  $\Delta d$  is the difference reading on the instrument between solution and solvent. The reading of total displacement,  $\Delta d$ , corrected for the solvent zero reading, is calculated as follows:

$$\Delta d = (d_2 - d_1) - (d_2' - d_1')$$

where  $(d_2 - d_1)$  is the reading of the solution,

and  $(d_2' - d_1')$  is the zero reading of the solvent (Fig. 2).

According to Bushuk and Benoit<sup>26</sup>, the specific refractive increment for binary copolymers expressed as a colligative property takes the form:

$$v = x_1 v_1 + (1 - x_1) v_2 \quad (1.17)$$

where  $v_1 = (dn/dc)_1$

$v_2 = (dn/dc)_2$

$v = (dn/dc)_{1.2}$

$x_1 = \frac{c_1}{c_1 + c_2}$ , the weight fraction of component 1,  
where  $c$  is g/mL.

Thus, according to equation (1.17), if the specific refractive increment for the two homopolymers is known in a given solvent, the weight fraction of both components can be calculated by determining  $v$  for the copolymer. The mole fraction can be calculated from the weight fraction through the following relationship:

$$F_1 = \frac{1}{1 + \left(\frac{x_2}{x_1}\right)\left(\frac{MW_1}{MW_2}\right)} \quad (1.18)$$

where  $MW_1$  and  $MW_2$  are the molecular weights of the two monomers.

#### Methods of Determining $r_1$ and $r_2$ Values

The experimental determination of  $r_1$  and  $r_2$  values involves polymerizing to low conversion for a variety of feed compositions. The polymers are isolated and their compositions are measured by one or more of the methods explained above.

Different methods of analyzing the data are available.

#### Direct Curve Fitting on Polymer-Monomer Composition Plots

In this method the mole fraction compositions of copolymers are plotted as a function of the monomer mixtures from which they are derived. Then the experimental points are placed on the graph and by trial and error, selection of  $r_1$  and  $r_2$  values for theoretical curves should result in a good fit of the experimental data in a few trials. As a guide  $1/r_1$  is equal to the initial slope of the composition curve at 100%  $M_1$  and  $1/r_2$  is equal to the slope of the curve at 100%  $M_2$ <sup>29</sup>.

This is a poor method, since the composition curve is rather insensitive to small changes in  $r_1$  and  $r_2$ .

### Intersecting Slopes Method

In this method  $r_1$  is allowed to take on selected values in the composition equation (1.13) for a single copolymer composition result and the corresponding  $r_2$  values are calculated by an equation derived from equation 1.13 shown below.

$$r_2 = \left( \frac{f}{1-f} \right)^2 \left( \frac{1-F}{F} \right) r_1 + \left( \frac{f}{1-f} \right) \left( \frac{1-2F}{F} \right)$$

$$\text{where } f = \frac{M_1}{M_1 + M_2}, \quad F = \frac{m_1}{m_1 + m_2}$$

$M_1$  and  $M_2$  are concentrations of monomer 1 and 2 in monomer mixture and  $m_1$  and  $m_2$  concentrations of monomer 1 and 2 in copolymer.

Calculated values of  $r_2$  are plotted as a function of  $r_1$ . Each experiment with a given feed composition gives a straight line, the region of intersection of several of these allows the evaluation of  $r_1$  and  $r_2$ . Because of the experimental errors, the lines generally do not intersect in a single point; the region within which the intersections occur gives some information about the precision of the experimental results.

### Fineman and Ross Method

The copolymerization equation (1.13) is rearranged to the form<sup>30</sup>.

$$\frac{g(G-1)}{G} = r_1 \frac{g2}{G} - r_2 \tag{1.19}$$

$$\text{where } g = \frac{M_1}{M_2}, \quad G = \frac{m_1}{m_2}$$

$M_1$  and  $M_2$  are concentration of monomer 1 and 2 in the monomer mixture and  $m_1$  and  $m_2$  concentration of monomer 1 and 2 in the copolymer.

A plot of  $g(G-1)/G$  as ordinate and  $g^2/G$  as abscissa will result in a straight line with a slope of  $r_1$  and an intercept of  $-r_2$ .

Equation 1.13 can also be rearranged as follows, in this case

$$\frac{G-1}{g} = -r_2 \frac{G}{g^2} + r_1 \quad (1.20)$$

slope is  $-r_2$  and the intercept is  $r_1$ .

The data can be plotted and a least squares method can be applied to determine the slope and intercept.

#### Kelen and Túdős Method

Kelen and Túdős<sup>31</sup> developed the linear equations 1.21 and 1.22.

$$\eta = \left( r_1 + \frac{r_2}{\alpha} \right) \zeta - \frac{r_2}{\alpha} \quad (1.21)$$

$$\text{and/or } \eta = r_1 \zeta - \frac{r_2}{\alpha} (1 - \zeta) \quad (1.22)$$

$$\text{where } \eta = \frac{g(G-1)/G}{\alpha + g^2/G}, \quad \zeta = \frac{g^2/G}{\alpha + g^2/G}$$

$G$  and  $g$  have the same meanings as used for Fineman-Ross Method. If  $X = g^2/G$  and  $X_m$  stands for the lowest and  $X_M$  for the highest values of the  $X$  values calculated from the series of measurements, then the choice of  $\alpha = \sqrt{X_m \cdot X_M}$  will afford optimum distribution of the data.

The  $\zeta$  cannot take any positive value, only those in the interval (0, 1). Thus plotting the  $\eta$  values calculated from the experimental data as a function of  $\zeta$ , one should obtain a straight

line, which extrapolated to  $\zeta=0$  and  $\zeta=1$  gives  $-r_2/\alpha$  and  $r_1$  (both as intercept).

### Quantitative Treatment of Composition Drift

A general formula for obtaining the copolymer composition for any conversion was developed by Skeist<sup>32</sup>.

He considered a mixture of two monomers, of mole fractions  $f_1$  and  $f_2$ , respectively. If the total amount of both monomers is  $M$  moles, then there are  $f_1M$  moles of the monomer 1 in the original monomer mixture. If  $dM$  moles of monomer polymerize, the number of moles of monomer 1 in the polymer is  $F_1dM$ , where  $F_1$  is mole fraction of monomer 1 in the copolymer. At the same time, the number of moles of monomer 1 in the monomer mixture has been reduced to  $(M-dM)(f_1-df_1)$ . The material balance of monomer 1 gives  $f_1M - (M-dM)(f_1-df_1) = F_1dM$ , and by neglecting the product of two differentials  $Mdf_1 + f_1dM = F_1dM$ , leading to  $dM/M = df_1/(F_1-f_1)$ . By integrating both sides, he obtained

$$\ln \frac{M}{M_0} = \int_{f_1^0}^{f_1} \frac{1}{F_1-f_1} df_1 \quad (1.23)$$

where  $M = M_1 + M_2$  and  $M^0 = M_1^0 + M_2^0$ .  $M$  is the total number of moles in monomer feed at a given time  $t$  of the copolymerization and  $M^0$  is the total number of moles in monomer feed at time zero. For given values of the reactivity ratios, graphical or numerical methods can be used to calculate the expected change in the monomer

mixture and copolymer composition corresponding to the mole conversion,  $1-M/M^0$ .

Initially the integral on the right side of equation (1.23) was usually evaluated numerically or graphically. For a binary copolymerization assuming only terminal unit effects Meyer and Lowry<sup>33</sup> have developed an analytical solution to Skeist's equation. Meyer and Lowry noted the equation for the instantaneous mole fraction  $F_1$  of monomer  $M_1$ , entering the copolymer from a binary monomer mixture containing  $f_1$  mole fraction of  $M_1$ ,

$$F_1 = \frac{(r_1-1)f_1^2 + f_1}{(r_1 + r_2-2)f_1^2 + 2(1-r_2)f_1 + r_2} \quad (1.24)$$

could be substituted into Skeist's equation and rearranged to obtain:

$$\ln \frac{M}{M_0} = \frac{1}{(2-r_1-r_2)} \int_{f_1^0}^{f_1} \frac{(r_1 + r_2-2)f_1^2 + 2(1-r_2)f_1 + r_2}{f_1(f_1-1) \left( f_1 - \frac{1-r_2}{2-r_1-r_2} \right)} df_1 \quad (1.25)$$

In this form the equation can be expanded and integrated to give,

$$\frac{M}{M_0} = \left( \frac{f_1}{f_1^0} \right)^\alpha \left( \frac{f_2}{f_2^0} \right)^\beta \left( \frac{f_1^0 - \delta}{f_1 - \delta} \right)^\gamma \quad (1.26)$$

where

$$\alpha = \frac{r_2}{1-r_2} \quad \gamma = \frac{1-r_1r_2}{(1-r_1)(1-r_2)}$$

$$\beta = \frac{r_1}{1-r_1} \quad \delta = \frac{1-r_2}{(2-r_1-r_2)}$$

$$f_1 = \frac{M_1}{M} = 1 - f_2 \quad r_1 = \frac{k_{11}}{k_{12}}; \quad r_2 = \frac{k_{22}}{k_{21}}$$

with the condition  $r_1 \neq 1$  and  $r_2 \neq 1$ .

Kruse<sup>34</sup> rearranged the form of the existing integrated copolymerization equation to a form that enables one to easily do the calculation of average copolymer composition versus extent of polymerization.

The copolymerization equation in its usual form is<sup>1</sup>:

$$\frac{dM_1}{dM_2} = \frac{M_1}{M_2} \cdot \frac{r_1 M_1 + M_2}{r_2 M_2 + M_1} \quad (1.27)$$

where  $M_1$  and  $M_2$  are the molar concentrations of the two monomers and  $r_1$  and  $r_2$  are the reactivity ratios. Equation 1.27 has been integrated by Mayo and Lewis<sup>3</sup> from initial values of  $M_1^\circ$  and  $M_2^\circ$  to values of  $M_1$  and  $M_2$  at any extent monomer conversion ( $p$ ) to yield:

$$\ln \frac{M_2}{M_2^\circ} = \frac{r_2}{1-r_2} \ln \frac{M_2^\circ M_1}{M_1^\circ M_2} - \frac{1-r_1 r_2}{(1-r_1)(1-r_2)} \ln \frac{(r_1-1)(M_1/M_2)-r_2+1}{(r_1-1)(M_1^\circ/M_2^\circ)-r_2+1} \quad (1.28)$$

Rearranging eq. (1.28) leads to eq. (1.29):

$$\left[ \frac{(1-r_1)M_1 - (1-r_2)M_2}{(1-r_1)M_1^\circ - (1-r_2)M_2^\circ} \right]^{1-r_1 r_2} = \left[ \frac{M_1}{M_1^\circ} \right]^{r_2 - r_1 r_2} \left[ \frac{M_2}{M_2^\circ} \right]^{r_1 - r_1 r_2} \quad (1.29)$$

Since the calculation of  $F_1$  as a function of  $p$  is difficult with the equation in this form, Kruse redefined the variables in eq. (1.29).

His definitions are listed below:

$f_1^\circ$  = the initial mole fraction of component one in the monomers

$f_1$  = final mole fraction of component one in the monomers

$f_2^\circ = 1 - f_1^\circ$

$f_2 = 1 - f_1$

$M_0$  = the total initial number of moles of both monomers

$(1-p)M_0$  = the number of moles remaining after an extent of reaction  $p$ . With these definitions:

$M_1^\circ = f_1^\circ M_0$

$M_2^\circ = f_2^\circ M_0$

$M_1 = f_1(1-p)M_0$

$M_2 = f_2(1-p)M_0$

By substituting these quantities in eq. (1.29) and rearranging them, one obtains:

$$(1-p)^{1+r_1r_2-r_1-r_2} = \left(\frac{f_1}{f_1^\circ}\right)^{r_2-r_1r_2} \left(\frac{f_2}{f_2^\circ}\right)^{r_1-r_1r_2} \left[\frac{(1-r_2)f_2^\circ - (1-r_1)f_1^\circ}{(1-r_2)f_2 - (1-r_1)f_1}\right]^{1-r_1r_2} \quad (1.30)$$

The extent of reaction  $p$  is now expressed as a function of the initial and final monomer mole fractions. This eq. (1.30) is equivalent to Meyer and Lowry's eq. (1.26).

From a component balance on the number of moles one can calculate  $F_1$ , the average polymer composition.

$$f_1^\circ M_0 - pF_1 M_0 = f_1(1-p)M_0 \quad (1.31)$$

Solving for  $F_1$ ,

$$F_1 = \frac{f_1^\circ - f_1(1-p)}{p} \quad (1.32)$$



For a given  $f_1^0$ ,  $r_1$  and  $r_2$ , the calculation procedure simply involves assuming a value of  $f_1$  and calculating a value of  $p$  with eq. (1.30) and then a corresponding value of  $F_1$  by eq. (1.32). By assuming various values of  $f_1$ , one can determine the complete curve of  $F_1$  versus  $p$ .

#### Goals of Current Research

Monomer reactivity ratios,  $r_1$  and  $r_2$ , of copolymers can be determined by various methods as seen in the above discussion. The goal of this research is to apply the methods to the very carefully conducted experimental copolymer composition data to evaluate the best  $r_1$  and  $r_2$  values and to see how well these calculation methods compare to each other.

In the literature there is a significant deviation in  $r_1$  and  $r_2$  values reported for the poly(styrene-co-methyl methacrylate) system. The  $r_1$  and  $r_2$  values seen below were obtained at 60.0°C by various workers using styrene as monomer one and methyl methacrylate as monomer two.

$r_1$	$r_2$	References
0.52 ± 0.026	0.46 ± 0.026	35
0.50 ± 0.02	0.50 ± 0.02	36
0.48	0.46	37
0.44 ± 0.08	0.50 ± 0.04	38
0.54 ± 0.04	0.42 ± 0.1	38
0.536 ± 0.02	0.50 ± 0.06	39

Since analysis of copolymer composition can be done with various methods, uncertainties in each method can lead to such deviations. Also use of different calculation methods to obtain monomer reactivity ratios,  $r_1$  and  $r_2$ , could be a possible source of these results. Another important fact is that in most studies the researchers do not consider the change in copolymer composition with changing degree of polymerization.

In this present work, the last two possible sources of deviation will be studied by evaluation of the composition drift equation to explain data at different conversions and comparison of monomer reactivity ratios obtained by different calculation methods. Results of these calculation methods will be compared to theoretically calculated values from the copolymer composition data using non-linear least squares fit to the Meyer-Lowry equation.

## CHAPTER II

### EXPERIMENTAL

#### Preparation of Low Conversion Styrene-Methyl Methacrylate Copolymers

Styrene and methyl methacrylate (both reagent grade, Fisher Scientific Company) were purified by distillation under low pressure immediately before use. Calcium metal was added before distillation. The center fraction (about 80%) of styrene was collected at 60°C and 45 torr. The center fraction (about 80%) of methyl methacrylate was collected at 35°C and 39 torr. The purity of the monomers was checked by gas chromatography and no impurities were found.

Polymerizations were done in sealed pyrex tubes, in a constant temperature bath. Each monomer was directly weighed into a narrow necked pyrex tube. After thorough mixing of the monomers, dibenzoyl peroxide (Aldrich Chemical Company, Inc.) 0.1% by mass of mixture was added as an initiator, the tubes were swept with nitrogen and were sealed under vacuum.

Nine groups of copolymerization mixtures were prepared. Each group contained eleven tubes, having 100, 90, 80, 70, 60, 50, 40, 30, 20, 10, and 0 mol % styrene. The total mass of the monomer mixture in each tube was approximately 10g.

The first group of each of the above concentrations of monomers was polymerized for one hour in a constant temperature water bath at  $60.0 \pm 0.1^\circ\text{C}$ . The second group was polymerized for two hours, the

third group for three, the fourth group for four, the fifth group for five, the sixth group for six, the seventh group for seven, the eighth group for eight, the ninth group for nine hours. At the end of the polymerization time, the eleven tubes belonging to each group were removed from the water bath and quickly cooled in dry ice.

#### Purification of Copolymers

Each copolymer was precipitated in 1000 to 1200 mL of methanol (Certified, Fisher Scientific Company) and the polymer was redissolved in 30 to 50 mL of methyl ethyl ketone (Certified, Fisher Scientific Company) and reprecipitated in 1200 to 1500 mL of methanol. The polymer then was filtered through quantitative filter paper (Whatman 42 ashless) with the aid of vacuum using a Buchner funnel and air dried.

Each copolymer sample was then dissolved in eight to ten times its mass of benzene (Analytical reagent, Mallinckrodt) in a flask and the solution was frozen in dry ice. The flask was then transferred to an ice bath and held at 0°C at 1-2 torr pressure to sublime the benzene from the polymer. About 40 to 45 hours were required for sublimation of most of the benzene. This frozen benzene technique<sup>40</sup> assures complete removal of solvent and unpolymerized monomers.

Removal of the remaining traces of solvents was completed by drying in a vacuum oven for 40 to 45 hours at 45°C and about 8-10 torr pressure. The conversion was determined by weighing.

The percent conversion values are given in Appendix B, Table I.

### Determination of Copolymer Composition

#### Method of Obtaining Refractive Index Increments

The refractive index increments were determined using a Brice-Phoenix differential refractometer, model BP-2000-V. This differential refractometer allows determination of the difference in refractive indices between a dilute solution and its solvent with a sensitivity of about  $\pm 0.000003$ .

The temperature can be controlled easily, because both the solvent and solution are examined simultaneously in a single cell, separated from each other by a thin diagonal glass partition. The ambient temperature need not be closely controlled since the temperature coefficient of the difference in refractive index between a solution and its solvent is much smaller than the temperature coefficient for the refractive index of solution or solvent alone. However, the solution and solvent in the differential cell should have the same temperature to within 0.01°C.

The instrument was calibrated by using solutions having known refractive index differences between solution and solvent. In the present work, distilled water solutions of potassium chloride at different concentrations were used as reference solutions. In

preparing the test solutions, potassium chloride (reagent grade, Fisher Scientific Company), was dried at approximately 90°C for 3-4 hours. The distilled water for all calibration solutions was taken from the same batch, because the instrument is sensitive enough to detect differences between water from different batches. Some of the distilled water used in preparing the solutions was retained for use as the reference solvent.

In the present work, the mercury green line (546nm) was used throughout and the instrument was calibrated to give the relationship;

$$\Delta n = 0.9144 \times 10^{-4} \Delta d.$$

In preparation of solutions of copolymer, methyl ethyl ketone (Fisher Scientific Company, A.C.S. Certified) and ethyl acetate (Fisher Scientific Company, A.C.S. Certified) were used as solvents. Samples of 0.0100g of each copolymer were dissolved in 10.0000g of solvent. In calculation of concentrations as g/mL, density vs. temperature graphs of each solvent were used<sup>41</sup>. For each sample the  $dn/dc$  value was calculated using the  $\Delta n$  value and the concentration. From these  $dn/dc$  values, the values of the mass fraction and the mole fraction of styrene in copolymer were calculated by using eq. (1.16 and 1.17).

These values can be seen in Appendix B, Table II.

### UV Absorption Spectra of Copolymers

Samples of the lowest conversion copolymers of each monomer feed composition were prepared by weighing out 10.0mg of polymer, dissolving it in chloroform (UV cut off 244nm, from Burdick & Jackson Laboratories, Inc.) and diluting to a concentration of 1.0mg/mL. The absorbance of each sample was determined at 269nm in a Beckman DU-6 Spectrophotometer.

Also solutions of these polymers were prepared in such a way that each sample had 1mg of styrene units per mL. The UV absorption spectra were obtained by a Hewlett Packard 8451 A Diode Array Spectrophotometer over the wavelength range of 240nm to 300nm.

## CHAPTER III

### RESULTS AND DISCUSSION

#### Results of Conversion Studies

The purpose of this study is to compare the calculation methods commonly used to obtain monomer reactivity ratios in free-radical copolymerization studies. Conversion versus time data can be seen in Appendix A, Table I and Appendix B, Table I.

At low conversions, which is the point of interest in this present work, an approximately proportional relationship between time and conversion to polymer was obtained as expected. Generally in first order kinetics the logarithm of conversion is plotted against time. In this study percent conversion versus time was plotted, as this way is used more frequently in polymer literature.

The following formulas<sup>42</sup> were used for estimating the proportionality constant from experimental values of  $x$  and  $y$  for the relationship  $y=mx$ .

$$m = \frac{\sum x_i y_i}{\sum x_i^2} \quad (3.1)$$

On these,

$m$  is the best value of the proportionality constant, slope.

$x_i$  is the time in hours, and

$y_i$  is the percent conversion.

$$\text{Also, } \sigma_y^2 = \frac{1}{(n-1)} (\sum y - m \sum x)^2 \quad (3.2)$$

where,  $\sigma_y$  is the estimated standard deviation of the  $y$ -residuals,



$n$  is the number of experimental points,  
and  $\sigma_m = \sigma_y \sqrt{1/\sum(x_i)^2}$  (3.3)

where,  $\sigma_m$  is the standard error of estimate of the slope.

For each monomer composition, the rate obtained by the slope of the percent conversion versus time plots and the standard error of the estimate of the slope, were calculated.

A plot of the rate of polymerization versus mole percent of styrene in the monomer mixture can be seen in Figure 3. The horizontal lines above and below the data points represent the standard error of estimate of the proportionality constants. The reverse J shape of the curve that was obtained is similar to the shape of similar plots given in the literature<sup>43</sup> by previous investigators.

As this subject is not the central point of interest in this study no further investigation has been done in this area. However, as the data were consistent with expectations and was available, it has been included to assist further researchers.

#### Copolymer Composition Studies With Refractive Index Increment Measurements

In this study the weight fraction and mole fraction of styrene in the copolymer is determined by refractive index increment measurements. The calculation method and formulas used are explained in the Introduction Chapter and their results can be seen in Appendix A, Table II.

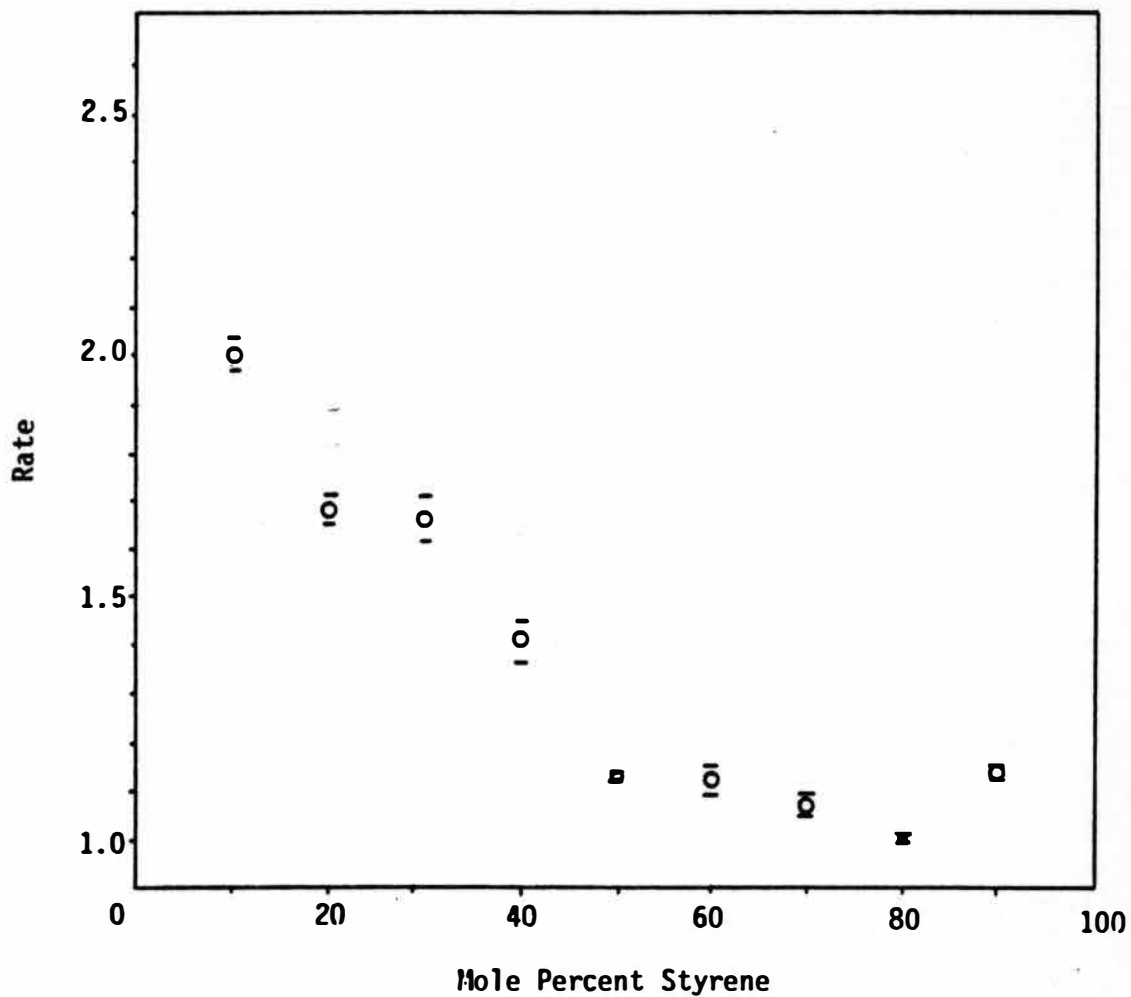


Figure 3. Rate of Copolymerization of Styrene and Methyl Methacrylate, in mole percent per hour, at  $60.0 \pm 0.1^\circ\text{C}$ . Horizontal bars represent standard error of estimate.

The average deviation and estimated standard deviation values can be calculated by,

$$\text{Average deviation} = \left| \frac{F_{MEK} - F_{EA}}{2} \right| \quad (3.4)$$

and,

$$\begin{aligned} \text{Standard deviation} &= \text{Average of average deviation} \times \sqrt{\pi/2} \quad (3.5) \\ &\approx \text{Average of average deviation} \times 1.25 \end{aligned}$$

where  $F$  is the mole fraction of styrene in copolymer in methyl ethyl ketone or ethyl acetate. These values can be seen below where  $f$  is the mole fraction of styrene in monomer mixture.

<u><math>f</math></u>	<u>Estimated Standard Deviation</u>
~ 0.1	0.001171
~ 0.2	0.000341
~ 0.3	0.000446
~ 0.4	0.000595
~ 0.5	0.000462
~ 0.6	0.001710
~ 0.7	0.001094
~ 0.8	0.000162
~ 0.9	0.000699

#### Evaluation of Methods of Estimating Reactivity Ratios from Experimental Data

##### Maximum Likelihood Method

The most probable values of parameters in a mathematical model based on the experimental data obtained were found by using a least squares computation.

The outcome of this computation will be valid if the model is correct and if there are no systematic errors in the data and no random errors in the independent values of  $f$  and conversion.

The best fit is found by computing the expected value of  $\hat{F}$  corresponding to each experimental value of  $f$  and the observed conversion. The difference between  $F$  and  $\hat{F}$  is the "residual" of the data point (i.e., it is the amount of apparent error remaining after computing the expected value).

This computation is done for all data points for a given assumed set of values of parameters,  $r_1$  and  $r_2$ . All the residuals for a particular set of  $r_1$  and  $r_2$  are squared and summed together to give the sum of squares of residuals, "SSR."

It can be shown by application of the probability theory that the best possible estimate of parameters consistent with the data set will be that set of values of  $r_1$  and  $r_2$  that gives a lower value of SSR than does any other set of parameter values. This is generally true whenever the random errors in the dependent variable ( $F$ ) are symmetrically distributed, e.g. normally distributed.

If SSR is plotted as a function of  $r_1$  and  $r_2$  on a three-dimensional Cartesian plot, the values form a surface that is approximately an elliptical paraboloid. The lowest value of SSR (the "least-squares" value) is at the vertex, or bottom tip of the paraboloid. This is true both in a linear equation such as  $y=mx+b$  and in more complex equations. The linear case equations can be solved algebraically to calculate the best values of  $m$  and  $b$ . When

the equations cannot be solved for more complicated cases, such as the present one, numerical calculations must be used to estimate the location of the minimum point on the SSR surface.

Various methods have been proposed and used. In this case a simple three by three grid search procedure is used, with the final grid spacing set at a value to yield five significant figures. By the nature of a grid search, the value obtained is not necessarily within the five-figure precision of the true minimum of the surface, but it probably is within four-figure precision, and almost certainly within three-figure precision. The value obtained in this way is used as the basis of comparison of other methods.

In this method the formulas of the Lowry and Meyer equation (1.26), together with a rearrangement of the Kruse equation (1.32), were used to compute the maximum likelihood values of  $r_1$  and  $r_2$ . The actual computations of SSR values were done with the aid of a computer program written by Dr. G. G. Lowry.

First, a particular set of values of  $r_1$  and  $r_2$  is chosen consisting of three values for each parameter. The initial choice is made with central values at one significant figure precision for both  $r_1$  and  $r_2$ . Then additional values of each parameter are chosen that are both larger and smaller than the central values. The amount of difference is 1 in the same decimal place location as the precision of the central values. Thus, choosing the central value of 0.5 for both  $r_1$  and  $r_2$  yields a 3 x 3 grid as follows:

		$r_2$		
		0.4	0.5	0.6
$r_1$	0.4			
	0.5			
	0.6			

Then for each of the nine points on this grid, the following procedure was used. The computer calculates the monomer composition at the experimentally determined conversion with the initial monomer composition and the assumed  $r_1$  and  $r_2$  values. For this calculation numerical values are given to solve the Meyer-Lowry equation. Then the average copolymer composition corresponding to these values is calculated. For this the material balance equation developed by Kruse is used. This copolymer composition is called the estimated copolymer composition. The residual is obtained by subtracting the estimated copolymer composition from the observed copolymer composition. Each residual is squared and the sum of these squared residual, SSR, is calculated. This calculation is reported for each of the nine assumed sets of  $r_1$  and  $r_2$  values.

Then the grid search method is used to obtain the best  $r_1$  and  $r_2$  values. In this method the calculation is started with the assumed  $r_1$  and  $r_2$  values that differ by an increment of 0.1 units. This estimation is based on literature values of similar studies. The objective is to obtain the smallest value for SSR in the middle box of this grid. If the smallest of the nine SSR values obtained thus is not in the middle square of the grid the  $r_1$  and  $r_2$  values that gave that value is placed in the middle of a new grid with the same

spacing of  $r_1$  and  $r_2$ . The calculation is continued until the smallest SSR value is in the center position.

Then the grid size is "shrunk" to one-tenth the initial spacing. The central values of  $r_1$  and  $r_2$  on the new, smaller grid are those that gave the smallest value of SSR with the initial grid size. The additional values of  $r_1$  and  $r_2$  are then greater and smaller than the central values by 0.01. Thus the original 3 x 3 grid has a spacing of 0.1, and the new, smaller grid has a spacing of 0.01. The computations of SSR are continued with this grid spacing until the lowest value of SSR corresponds to the central  $r_1$  and  $r_2$  values for a grid. The process is repeated with grid spacings of 0.001, then 0.0001, and finally 0.00001.

The  $r_1$  and  $r_2$  values at five significant figures that corresponds to this smallest SSR are then accepted as the best  $r_1$  and  $r_2$  values that will be used as a base for comparison of different methods of finding  $r_1$  and  $r_2$ . The other methods which are discussed next were used to estimate  $r_1$  and  $r_2$  to a precision of five significant figures for comparison. The best fit (maximum likelihood) values of reactivity ratios,  $r_1$  and  $r_2$ , are found to be 0.49520 and 0.46669 respectively.

This method however is tedious and lengthy even with a computer. Therefore, it is desirable to find a simpler method that will give estimates of  $r_1$  and  $r_2$  as close as possible to these values. A contour plot (Fig. 4) serves as one criterion of evaluating how good the other fitting methods are.

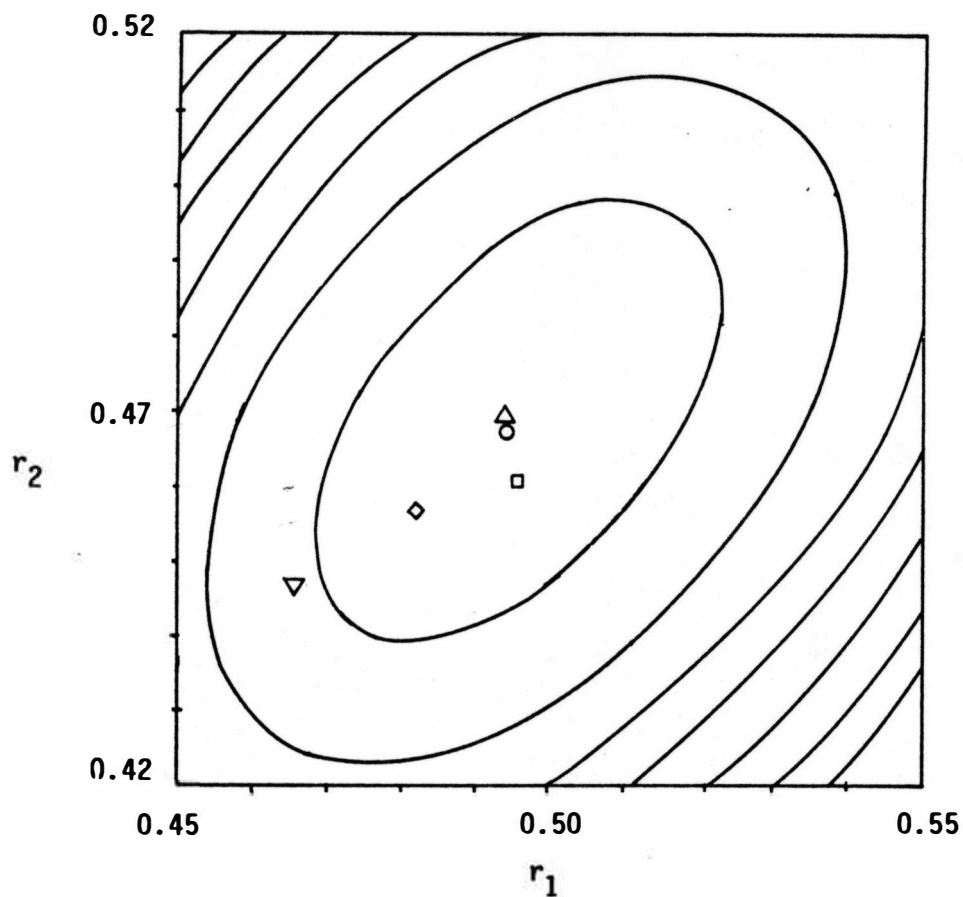


Figure 4. Contours Representing Surface of Residuals-Squared for Non-Linear Least Squares Fitting of Weighted Styrene-Methyl Methacrylate Copolymer Data. Points Represent Different Methods of Evaluation, Maximum Likelihood ( $\Delta$ ), Non-Linear Least Squares ( $\circ$ ), Intersection ( $\square$ ), Kelen-Tüdös Method ( $\diamond$ ), Fineman-Ross ( $\nabla$ ).



To draw the contour plot, the values are computed at SSR at many coordinates of  $r_1$  and  $r_2$  and are interpolated to find coordinates of points with same values of SSR. Then contour lines are plotted through these calculated points. The value of SSR at the minimum according to this method was 0.003772.

#### Methods Using Extrapolated Zero-Conversion Data

As seen in Figure 5 the  $F$  versus conversion lines show no significant curvature over the range of conversions studied. Thus for a simpler computational method, all  $F$  values for each  $f$  value were fitted by ordinary linear least squares to obtain the intercept with its uncertainty. This value corresponds to zero-conversion extrapolated values, that is, to the instantaneous copolymer composition to which the Mayo equation applies. Then for each method a single data point for each monomer composition is used.

The uncertainty of  $F$  is available from the ordinary linear least squares fit. In the calculation of each average value of  $f$ , the values for a set of data are very close to each other but not identical because of instrumental and equipment limitations. In calculations the average  $f$  values were used and their uncertainties were included in the method of intersections.

Whenever "weighted" data are referred to in the following sections, the weighting factors are the reciprocals of the squares of the uncertainties of individual values. Sometimes the weighting

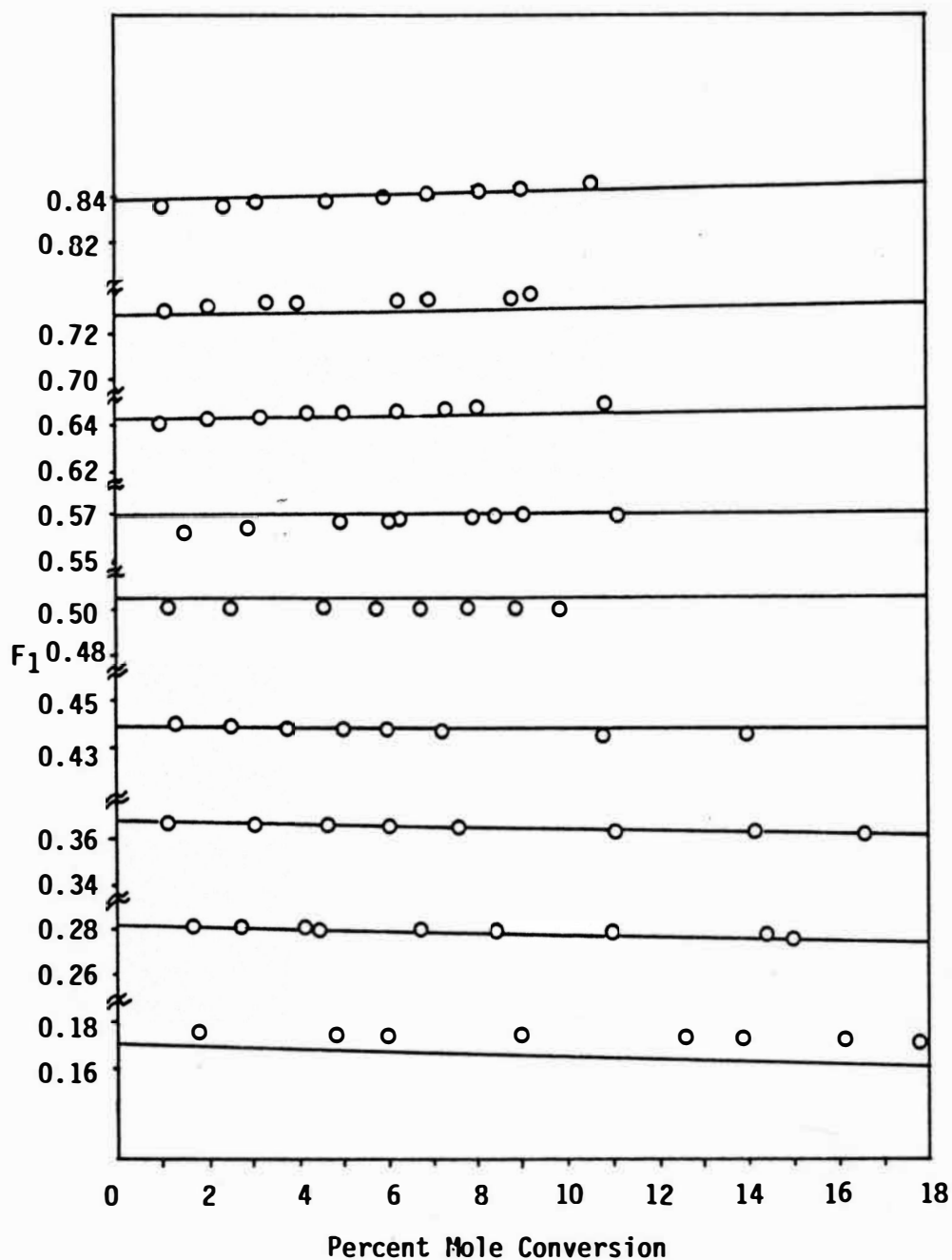


Figure 5. Mole Fraction of Styrene in Copolymer Mixture ( $F_1$ ) Versus Percent Mole Conversion. Circles Represent Actual Data Points, Solid Lines are Calculated Results Assuming  $r_1=0.495$  and  $r_2=0.467$ .

factors are multiplied by a scaling factor, but that does not change the outcome of the results.

Formulas used in these calculations are as follows. For all points with the same initial monomer composition,

$$\bar{f}_1^\circ = \frac{1}{n} \sum f_1^\circ \quad (3.6)$$

where  $f_1^\circ$  is the initial monomer composition,

$n$  is the number of samples, and

$\bar{f}_1^\circ$  is the average initial monomer composition.

Furthermore,

$$\sigma_{f_1^\circ} = \sqrt{\frac{\sum (f_1^\circ - \bar{f}_1^\circ)^2}{n-1}} \quad (3.7)$$

where  $\sigma_{f_1^\circ}$  is the standard deviation of  $f_1^\circ$ .

The uncertainty (95% confidence limits) of  $\bar{f}_1^\circ$  is

$$\Sigma_{f_1^\circ} = \frac{\sigma_{f_1^\circ}}{\sqrt{n}} \cdot t_{0.95} \quad (3.8)$$

where  $t_{0.95}$  is the student's  $t$  value for 95% confidence and for the number of values used in the calculation of  $\bar{f}_1^\circ$ .

Using a least squares fit,  $F_1$  versus mole percent conversion was plotted for each monomer composition and  $\hat{F}_1^\circ$  was obtained from intercept.

$\hat{F}_1^\circ$  is the estimated instantaneous copolymer composition,

$\sigma_{F_1^\circ}$  is the standard error of the intercept,

and the uncertainty (95% confidence limits) of  $\hat{F}_1^\circ$  is

$$\Sigma_{F_1^\circ} = \sigma_{F_1^\circ} \cdot t_{0.95} \quad (3.9)$$

### Nonlinear Least Squares

Using the values of  $\overline{f_1}^\circ$  and  $\widehat{F_1}^\circ$ , obtained above, a 3 X 3 grid search yielded the data listed below.

Table 1  
Copolymer Composition Data Using Weighted  
Nonlinear Least Squares

$f$	$F_1$ (observed)	Weight	$F_1$ (calculated)	residual
0.10018600	0.17596100	0.02428480	0.16857200	-0.00738952
0.20009900	0.28244800	0.11501100	0.28131800	-0.00113018
0.30002100	0.36719200	0.19784700	0.36687300	-0.00031942
0.40001300	0.43987100	0.05462130	0.43868200	-0.00118898
0.49999900	0.49993900	0.14987800	0.50459400	0.00465441
0.60003000	0.56365300	0.02182560	0.57054700	0.00689381
0.69998800	0.64100000	0.02936130	0.64228000	0.00128060
0.79999100	0.72996400	0.30681000	0.72743600	-0.00252816
0.89999100	0.83524100	0.10036100	0.83838900	0.00314707

### Intersection Method

In this method as explained in the Introduction Chapter locating the best values of  $r_1$  and  $r_2$  from the "probable area" confined by different straight lines on the  $r_1$  versus  $r_2$  plot is done using the subjective judgment of the observer. This judgment introduces a source of an undetermined amount of error. To overcome this difficulty, in this present work the weighted average values of  $r_1$  and  $r_2$  computed from all possible intersections of pairs of lines is used. The calculation of the uncertainties of these weighted averages does provide an objective measure of the degree of precision in the experimental data. Figure 6 shows the  $r_1$  versus  $r_2$  plots in which the nine lines representing the nine values of  $\overline{f_1}^\circ$  and  $\widehat{F_1}^\circ$  are numbered.

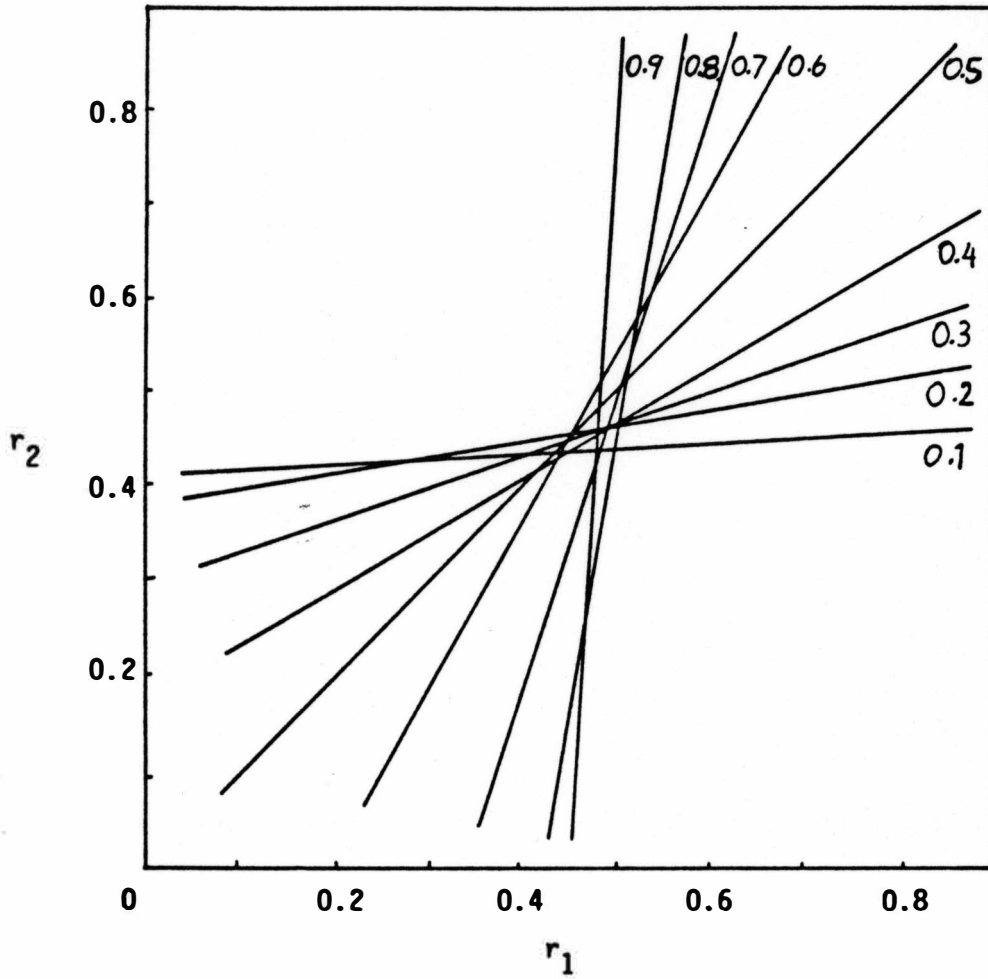


Figure 6. Illustration of the Application of the Intersection Method to the Data of Table 1. The Values on the Figure are Approximate Monomer Compositions, Actual Compositions are Given in Table 1.

To estimate the uncertainties in  $r_1$  and  $r_2$  values of the various points of intersection on this graph, it was first necessary to obtain the uncertainties of the  $\bar{f}_1^\circ$  and  $\hat{F}_1^\circ$  data points as described earlier.

Each of the lines in Figure 6 is plotted using the following equation, with zero-concentration extrapolated values,  $\hat{F}_1^\circ$  and  $\bar{f}_1^\circ$  of  $F$  and corresponding  $f$  inserted for each line. The  $r_1$  and  $r_2$  values for each intersection point were calculated using the following formulas.

$$r_2 = \left( \frac{f_1}{1-f_1} \right)^2 \left( \frac{1-F_1}{F_1} \right) r_1 + \left( \frac{f_1}{1-f_1} \right) \left( \frac{1-2F_1}{F_1} \right)$$

where  $f_1$  is the mole fraction of styrene in monomer mixture, and  $F_1$  is the mole fraction of styrene in copolymer.

This straight line equation can be represented by the simpler form

$$r_2 = ar_1 + b.$$

The uncertainties of  $a$  and  $b$  for each line were calculated using the usual form for computing propagated error in derived quantities. In this case,

$$\epsilon_a = \left[ \left( \frac{\partial a}{\partial f^\circ} \right)^2 \epsilon_{f_1^\circ}^2 + \left( \frac{\partial a}{\partial F_1^\circ} \right)^2 \epsilon_{F_1^\circ}^2 \right]^{1/2}$$

$$\epsilon_b = \left[ \left( \frac{\partial b}{\partial f^\circ} \right)^2 \epsilon_{f_1^\circ}^2 + \left( \frac{\partial b}{\partial F_1^\circ} \right)^2 \epsilon_{F_1^\circ}^2 \right]^{1/2}$$

For the intersection of each pair of lines  $i$  and  $j$ ,

$$r_1 = \frac{bj - bi}{ai - aj} \quad \text{and} \quad r_2 = \frac{aibj - ajbi}{ai - aj}$$

and the uncertainties of these values are given by

$$\epsilon_{r_1} = \frac{1}{|a_i - a_j|} \left[ \epsilon^2_{b_i} + \epsilon^2_{b_j} + r_1^2 (\epsilon^2_{a_i} + \epsilon^2_{a_j}) \right]^{1/2}$$

$$\epsilon_{r_2} = \frac{1}{|a_i - a_j|} \left[ a_i^2 \epsilon^2_{b_j} + a_j^2 \epsilon^2_{b_i} + r_1^2 (a_j^2 \epsilon^2_{a_i} + a_i^2 \epsilon^2_{a_j}) \right]^{1/2}$$

The values of the coordinates of all the intersection points in Figure 6, together with their uncertainties, are given in Table 2.

Each of the intersecting lines has a band of uncertainty associated with it which can be represented by parallel lines. Actually the outer lines of the band are curved rather than straight, but over a short range they are approximately straight. For example, with two extreme cases, the intersecting lines with their uncertainty bands might be as shown below. The uncertainty bands are labelled as U, and the maximum uncertainty region of the intersection point is represented by the cross-hatched square or rectangle.

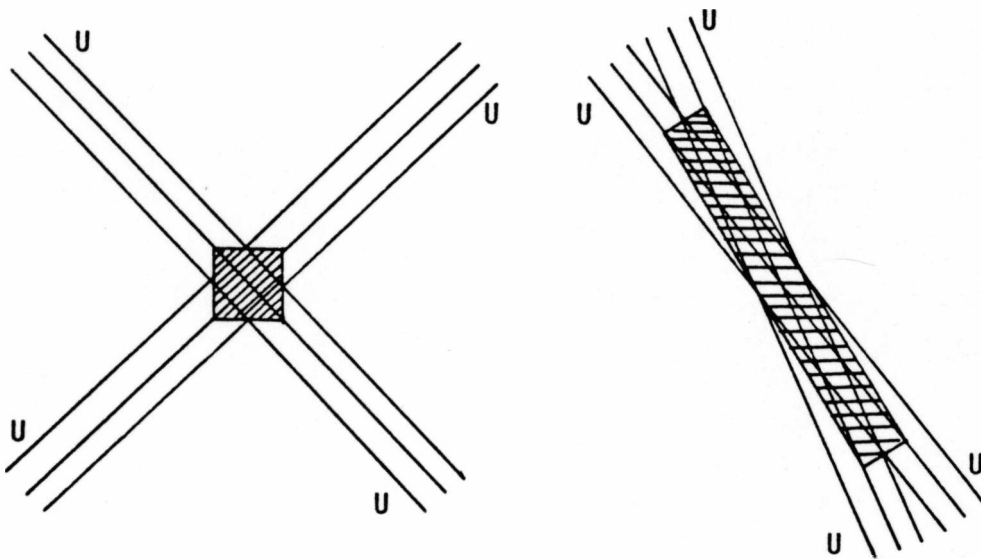


Table 2  
 Monomer Reactivity Ratios and Uncertainties  
 at Each Intersection Point

Intersecting lines	$r_1$	$\epsilon_{r_1}$	$r_2$	$\epsilon_{r_1}$
1-2	0.2475	0.0491	0.4244	0.0073
1-3	0.3869	0.0186	0.4325	0.0056
1-4	0.4485	0.0108	0.4361	0.0051
1-5	0.4350	0.0054	0.4353	0.0049
1-6	0.4447	0.0052	0.4359	0.0048
1-7	0.4803	0.0036	0.4380	0.0047
1-8	0.5000	0.0013	0.4391	0.0046
1-9	0.4796	0.0022	0.4379	0.0046
2-3	0.4759	0.0147	0.4607	0.0039
2-4	0.4982	0.0087	0.4643	0.0028
2-5	0.4574	0.0034	0.4578	0.0022
2-6	0.4573	0.0049	0.4578	0.0021
2-7	0.4884	0.0035	0.4627	0.0020
2-8	0.5044	0.0011	0.4652	0.0019
2-9	0.4811	0.0022	0.4615	0.0019
3-4	0.5123	0.0135	0.4722	0.0051
3-5	0.4532	0.0039	0.4535	0.0023
3-6	0.4552	0.0054	0.4542	0.0030
3-7	0.4892	0.0036	0.4649	0.0020
3-8	0.5052	0.0011	0.4700	0.0018
3-9	0.4812	0.0023	0.4624	0.0016
4-5	0.4192	0.0086	0.4195	0.0075
4-6	0.4431	0.0069	0.4331	0.0057
4-7	0.4868	0.0041	0.4578	0.0043
4-8	0.5049	0.0012	0.4681	0.0034
4-9	0.4807	0.0023	0.4543	0.0034



Table 2 -- Continued

Intersecting lines	$r_1$	$\epsilon_{r_1}$	$r_2$	$\epsilon_{r_2}$
5-6	0.4570	0.0017	0.4574	0.00115
5-7	0.5012	0.0050	0.5015	0.0059
5-8	0.5125	0.0013	0.5128	0.0030
5-9	0.4824	0.0024	0.4828	0.0034
6-7	0.5262	0.0100	0.5778	0.0231
6-8	0.5223	0.0024	0.5711	0.0120
6-9	0.4838	0.0026	0.5039	0.0097
7-8	0.5206	0.0042	0.5607	0.0221
7-9	0.4795	0.0028	0.4354	0.0020
8-9	0.4677	0.0035	0.2480	0.0219

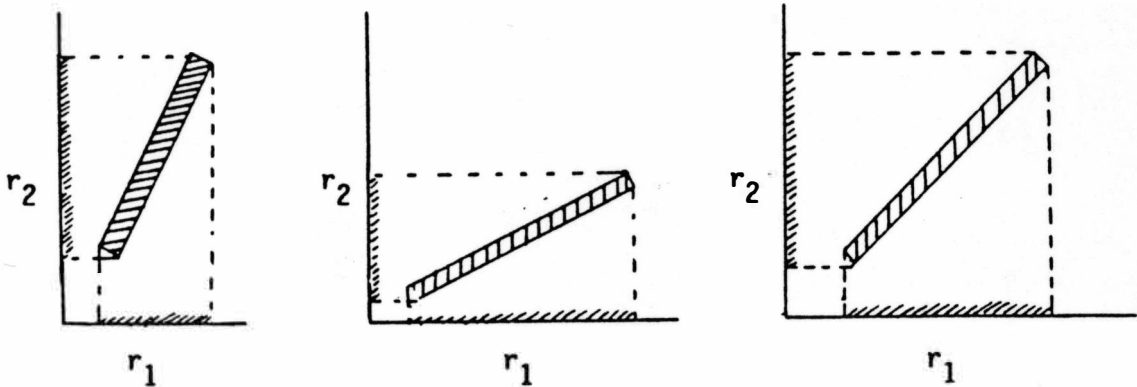
Thus in these two cases in which all the lines have the same width of uncertainty band, there is an extremely large difference in the size and shape of the uncertainty region of intersection.

Any time the two lines are not at right angles to each other, the uncertainty region is a rectangle (or perhaps an ellipse) whose long axis coincides with a line that bisects the smaller angle of the intersection. The length of the long axis of the region in the example is much greater than that of the short axis.

Then the relative uncertainties of the  $r_1$  and  $r_2$  values depend not only on the angle at which the lines intersect, but also on the angle the line of bisection make with the  $r_1$ ,  $r_2$  axes.

The following figures illustrate this concept where the uncertainties on each axis are shadowed. It is seen that the relative uncertainties of  $r_1$  and  $r_2$  of intersection are very

different for these three cases involving identical size and shape of the uncertainty regions of intersection.



It can be seen from Table 2 that  $r_1$  and  $r_2$  values vary from 0.2475 to 0.5262 and 0.2480 to 0.5778 respectively. The procedure commonly used in the past has been to decide from the visual appearance of a graph such as Figure 6 the most likely set of values and their uncertainties for  $r_1$  and  $r_2$ . However, by calculating the results in Table 2 it is possible to obtain the final results in a more objective way. Thus the weighted average of  $r_1$  and  $r_2$  values ( $\bar{r}_1$  and  $\bar{r}_2$ ) are found from the following formulas,

$$\frac{\sum \left( \frac{r_1}{\epsilon_{r_1}^2} \right)_{i,j}}{\sum \left( \frac{1}{\epsilon_{r_1}^2} \right)_{i,j}} = \bar{r}_1 \quad \text{and} \quad \frac{\sum \left( \frac{r_2}{\epsilon_{r_2}^2} \right)_{i,j}}{\sum \left( \frac{1}{\epsilon_{r_2}^2} \right)_{i,j}} = \bar{r}_2$$

The uncertainty in  $\bar{r}_1$  and  $\bar{r}_2$  values are found using the following equations for the case of  $\bar{r}_1$ , and similar equations for  $\bar{r}_2$ .

$$\hat{\sigma}_{r_1} = \left[ \frac{K \sum \frac{1}{\epsilon_{r_1}^2} \left[ r_{1,i,j} - \bar{r}_1 \right]^2}{n-1} \right]^{1/2}$$

where,  $\hat{\sigma}_{r_1}$  is the standard error

$$n = K \sum \frac{1}{\epsilon_{r_1}^2}$$

and  $\hat{\epsilon}_{r_1} = \frac{\hat{\sigma}_{r_1}}{\sqrt{n}} \cdot t_{0.95}$

where,  $\hat{\epsilon}_{r_1}$  is the uncertainty of error of  $r_1$

$n$  is the number of intersection points.

By applying the above equations to the values in Table 2, the weighted average values of  $\bar{r}_1$  and  $\bar{r}_2$  and absolute error in 95% confidence limits were found to be  $0.49581 \pm 0.00592$  and  $0.46037 \pm 0.00579$ , respectively.

Although  $r$  values are estimated to the precision of three significant figures they are stated to five significant figures for comparison between methods.

#### Fineman and Ross Method

As is illustrated in the Introduction Chapter, in this method the copolymerization equation (1.13) is rearranged to the form of

$$\frac{g}{G} (G-1) = r_1 \frac{g^2}{G} - r_2 \quad (1.19)$$

where  $g = \frac{M_1}{M_2}$ ,  $G = \frac{m_1}{m_2}$

A plot of  $g/G (G-1)$  as the ordinate and  $g^2/G$  as the abscissa is a straight line whose slope is  $r_1$  and whose intercept is  $-r_2$ . The uneven spacing of the data points can clearly be seen in Figure 7a and 7b. Results of the least squares calculations using equation 1.19 are

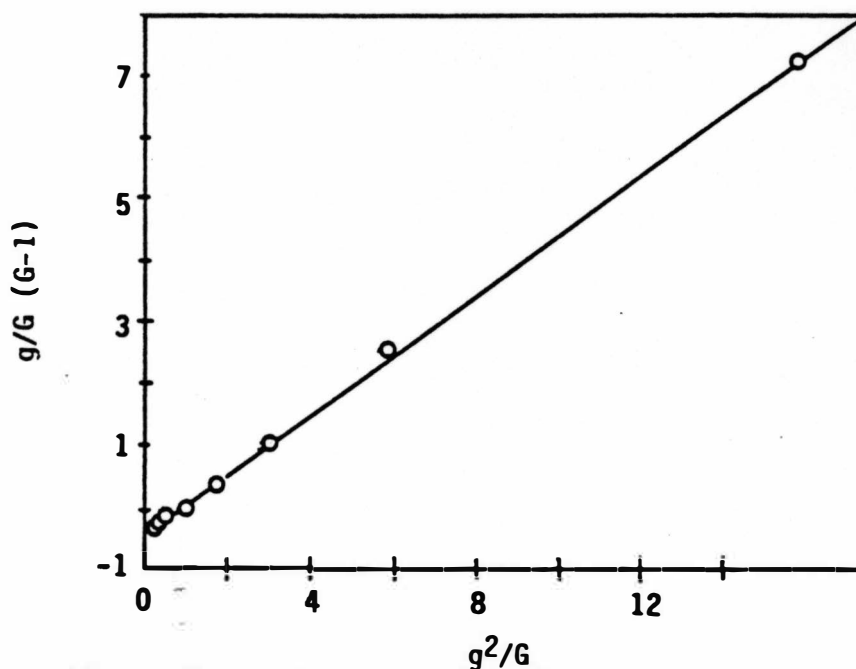


Figure 7a. Fineman-Ross Method using Equation 1.19, Styrene as Monomer 1.

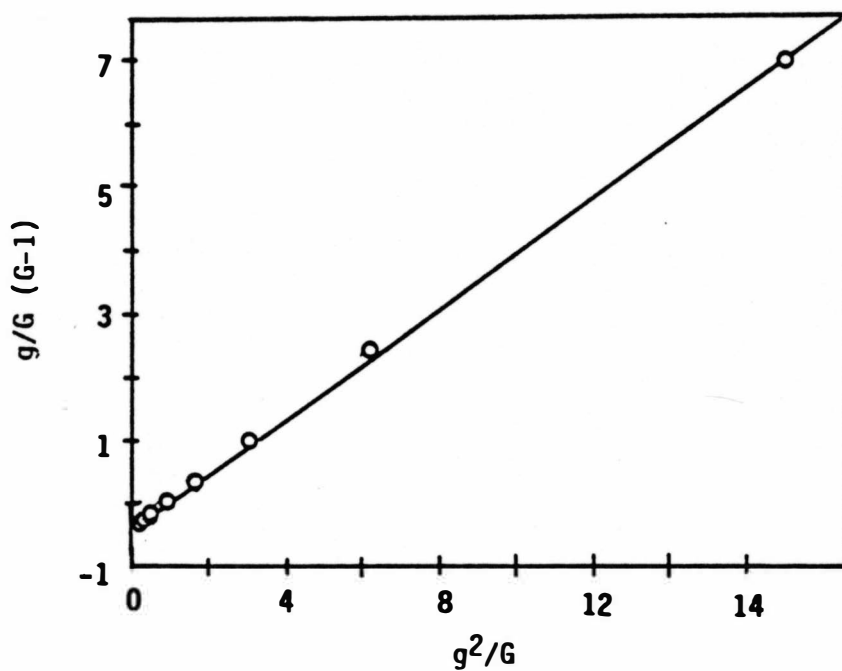


Figure 7b. Fineman-Ross Method using Equation 1.19, Methyl Methacrylate as Monomer 1.

Monomer 1	$r_1$	$r_2$
Styrene	0.48286024	0.45303593
Methyl methacrylate	0.43888575	0.44871682

Equation (1.13) can also be rearranged to the form of

$$\frac{G-1}{g} = -r_2 \frac{G}{g^2} + r_1 \quad (1.20)$$

In this case the slope is  $-r_2$  and the intercept is  $r_1$ . There is also uneven spacing of the data points on the plot drawn by using equation 1.20. This can be seen in Figures 8a and 8b. The results of using equation 1.20 are

Monomer 1	$r_1$	$r_2$
Styrene	0.44872683	0.43888595
Methyl methacrylate	0.45303557	0.48285998

According to Fineman and Ross<sup>30</sup>, data can be plotted and a least squares method can be applied to determine the slope and intercept in both cases. The values of  $r_1$  and  $r_2$  determined by plotting in term of equation 1.19 and 1.20 should be in excellent agreement.

It is common practice to give the average values of  $r_1$  and  $r_2$  for the two cases where monomer one is styrene and monomer one is methyl methacrylate. For this case these values can be seen below.

Average results from	$r_1$	$r_2$
Eq. 1.19	0.46578853	0.44596584
Eq. 1.20	0.46579341	0.44596076
Overall	0.46579097	0.44596330

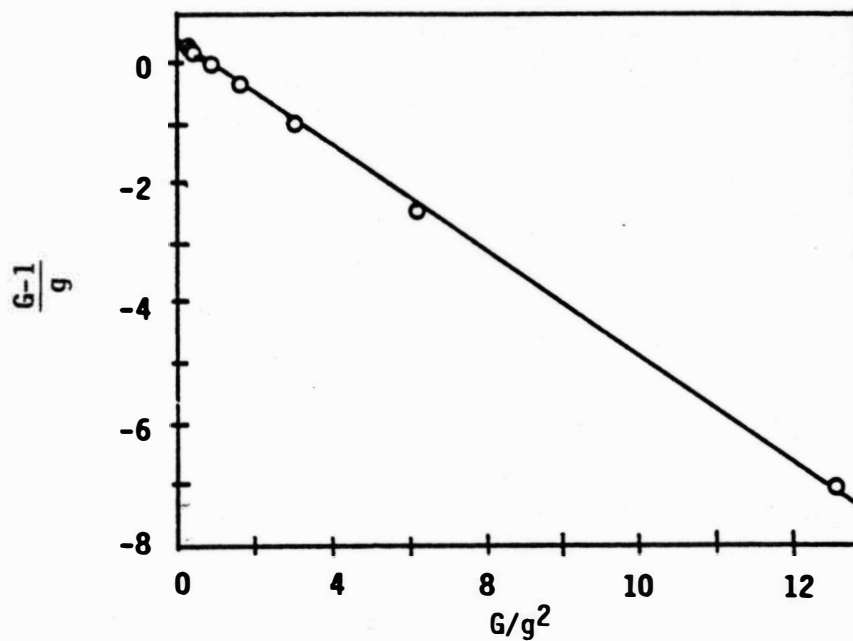


Figure 8a. Fineman-Ross Method using Equation 1.20, Styrene as Monomer 1.

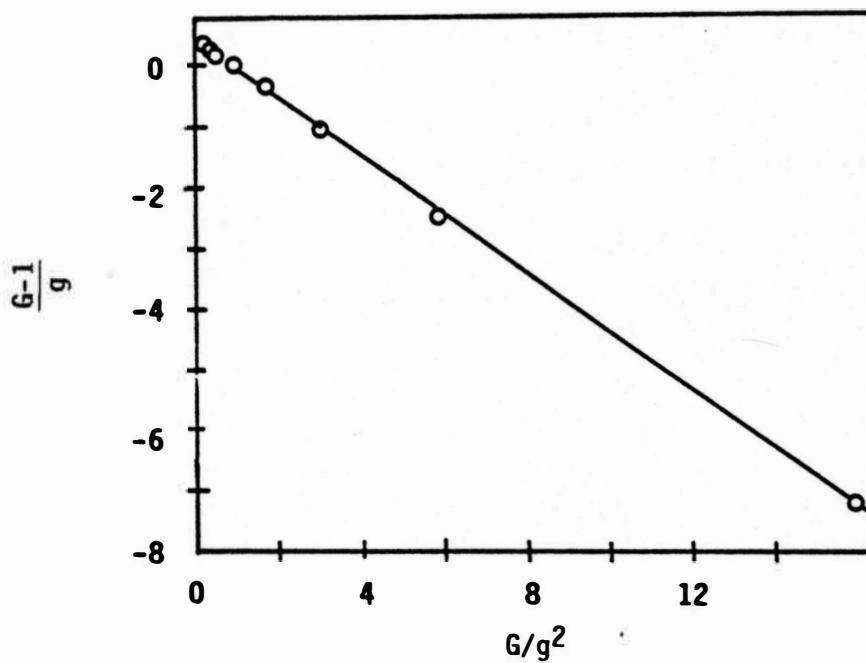


Figure 8b. Fineman-Ross Method using Equation 1.20, Methyl Methacrylate as Monomer 1.

### Kelen and Túdős Method

Kelen and Túdős introduced a new improved linear graphic method to calculate  $r_1$  and  $r_2$  values. They modified the Fineman-Ross equation (1.19) by adding a parameter,  $\alpha$ , into the formula of the straight line. The resulting straight line gives both  $r_1$  and  $r_2$  values as intercepts. This method has been explained in detail in the Introduction Chapter.

Experimental results of using this method are shown in Figures 9a and 9b. The results of the least squares computations from these graphs are

Monomer 1	$r_1$	$r_2$
Styrene	0.482306608	0.456037653
Methyl methacrylate	0.455225229	0.481477279

It is seen that the result of reversing indices or monomers are much more consistent than in the Fineman-Ross method. Also in these plots the data points are distributed much more uniformly along the abscissa.

The two sets of results are not identical because of the experimental errors in both variables of the linearized equation. However, their differences are small, and the averages of the two computations are probably more reliable. These values are,  $r_1 = 0.481891944$  and  $r_2 = 0.455644972$ , where monomer one is styrene.

### Effect of Composition Drift With Conversion

The method of extrapolating to zero conversion prevents a drift in values. To show this effect Kelen and Túdős non-zero conversion values were calculated by using about 5% conversions for low

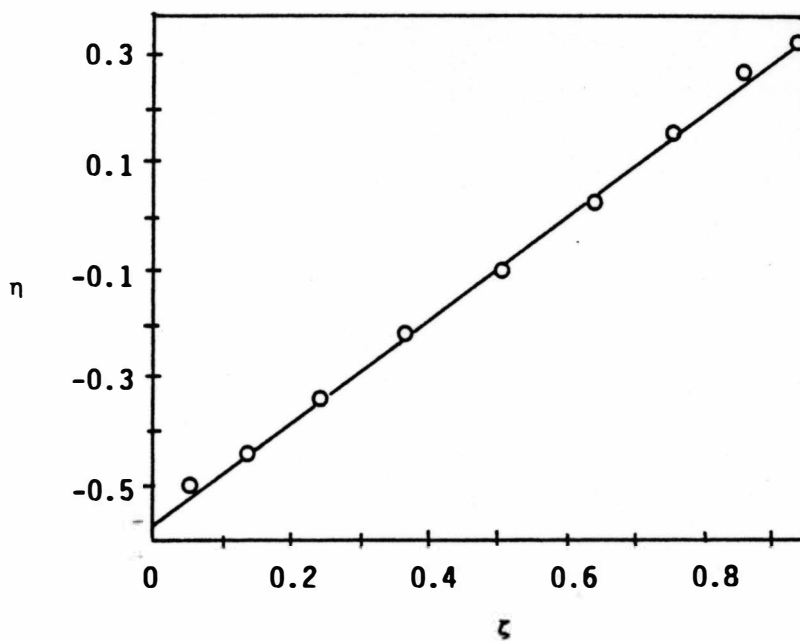


Figure 9a. Kelen-Tüdös Method, Styrene as Monomer 1.

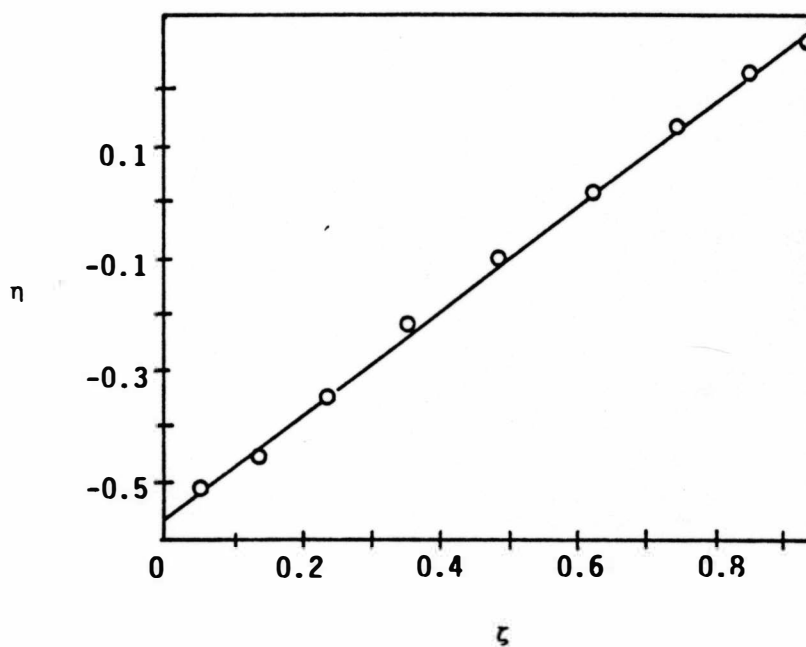


Figure 9b. Kelen-Tüdös Method, Methyl Methacrylate as Monomer 1.



conversion and about 9 to 18% conversion for the high conversion. For the approximately 5% conversion an average of the conversions of samples 4.8595, 4.6263, 4.6763, 5.0365, 5.1957, 5.0229, 5.0461, 5.2891, and 4.7341 was used. For the approximately 9 to 18% conversion average of the conversion of samples 17.8377, 15.0423, 16.6655, 9.8882, 11.2064, 9.2946, 10.6556, 10.8991, and 14.0397 was used.

Conversion	$r_1$	$r_2$
~ 5%	0.495474564	0.467087760
~ 9 to 18%	0.521593058	0.491053178

#### Comparison of Methods and Discussion

In this study the various methods summarized in Table 3 are compared with  $r_1$  and  $r_2$  values obtained using a two dimensional grid search as described earlier in this section.

Actually there are five methods for finding the monomer reactivity ratios. The one that was not considered in this study but was explained in the Introduction Chapter is the direct curve fitting on polymer-monomer composition plot. This method has two big disadvantages. One is that it is not sensitive to small changes in monomer reactivity ratios. The other is the large uncertainty, of the slope of the tangent drawn to the curves at  $f_1 = 0$  and  $f_1 = 1$  to find  $1/r_2$  and  $1/r_1$  values. In this study however non-linear least squares fit method was tested using the curve in Figure 10 obtained by plotting the instantaneous composition of copolymer,  $F_1$ , versus monomer composition,  $f_1$ . The data points obtained using  $r_1$

Table 3  
Comparison of Methods

Computation Method	$r_1$	$r_2$	SSR
Maximum Likelihood	0.49520	0.46669	0.003772
Extrapolated Zero-Conversion:			
Non-Linear Least Squares	0.49533	0.46810	0.003787
Intersection	0.49581	0.46037	0.004046
Fineman-Ross	0.46579	0.44596	0.008716
Kelen and Túdős	0.48189	0.45564	0.004795
Non-Zero Conversions: (by Kelen-Túdős)			
~ 5%	0.49547	0.46709	0.003774
~ 9 to 18%	0.52159	0.49105	0.007819

and  $r_2$  values from the non-linear least squares method has fitted this curve without any visually noticeable deviation.

In this study, the various methods are compared with obtained  $r_1$  and  $r_2$  values using a two dimensional grid search as described in Maximum Likelihood Method. The  $r_1$  and  $r_2$  values obtained with the four different methods are shown all together on the graph seen in Figure 4. This figure was obtained by doing the SSR calculation on a grid basis and the calculated contour lines of equal SSR values were plotted, using interpolation between calculated levels of SSR.

The best method is the Non-Linear Least Squares Method that gives a point almost at the center of the ellipsoid contour.

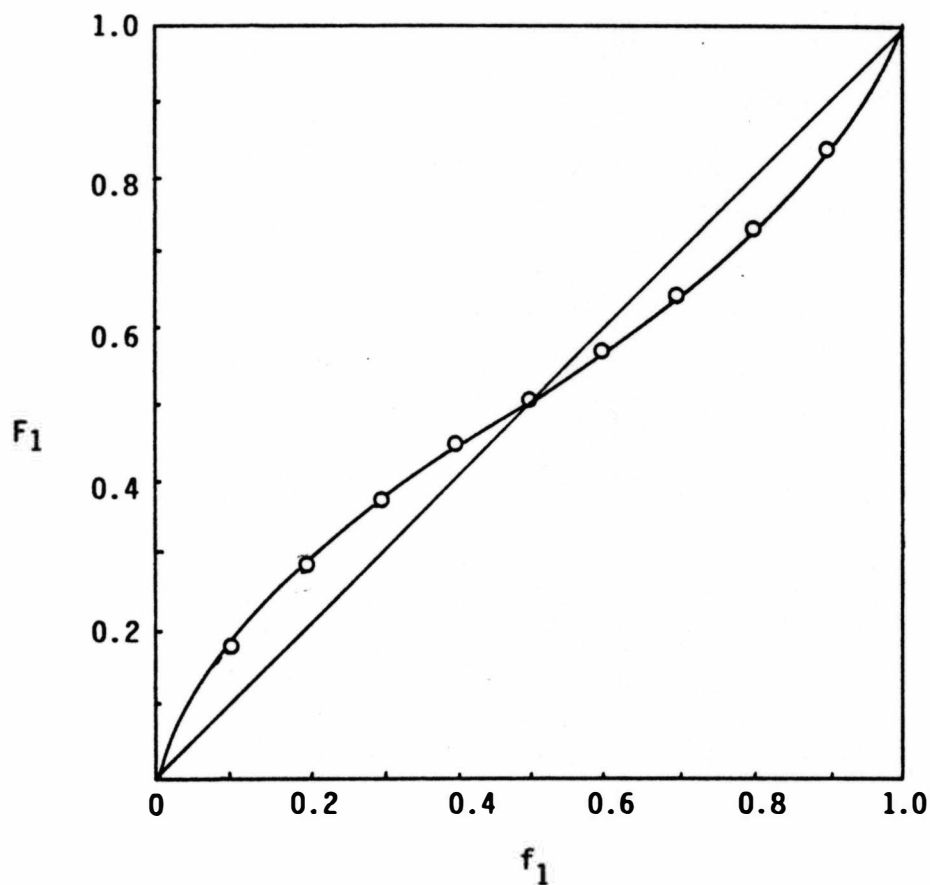


Figure 10. Instantaneous Composition of Copolymer  $F_1$  as a Function of Monomer Composition  $f_1$  for the Values of Reactivity Ratios,  $r_1$  and  $r_2$ , 0.495 and 0.467. Circles Represent Copolymer Composition Extrapolated to Zero Conversion, Solid line is Calculated value.

However the following conditions must be met for the accuracy of this method.

1. The mathematical model, a combination of the Mayo equation and the Meyer-Lowry equation, is correct.
2. There are no systematic errors in analysis of the polymers for their composition.
3. There are no systematic errors in the determination of the conversion of the polymers.
4. There are only random errors in the copolymer composition.
5. Any systematic errors present are negligibly small.

In the Fineman-Ross and Kelen-Túdős methods the non-linear form of the Mayo equation is linearized to fit a straight line to the adjusted data. This linearization reduces the accuracy of the results calculated by these methods in two ways. First, it distorts the error structure so that even though all the original data points may have the same uncertainty, the errors of the adjusted values that are plotted are not the same. Secondly, this adjustment of data introduces uncertainty in both abscissa and ordinate data even though in the original data there is no uncertainty in abscissa values. Ordinary least squares calculations are applied to these methods, but the ordinary least squares method assumes no error in abscissa and equal uncertainty of all data points. Furthermore the original data are uniformly spaced along the horizontal axis.

The Fineman-Ross method distorts the data so that some of the resulting adjusted values have a greater influence on the slope and intercept of the line than they should. Therefore, the largest deviation is seen in the Fineman-Ross method using the equation 1.19 and 1.20. Indeed it can easily be seen that  $r_1$  and  $r_2$  values obtained by applying the same experimental data to equation 1.19 and 1.20 gives different results. Also, different  $r_1$  and  $r_2$  values are obtained in cases where calculations are made using styrene as  $M_1$  in one case and methyl methacrylate as  $M_1$  in the other case.

The Kelen-Túdős method avoids the problem of unbalanced weighting of some points. The data points are spread so that they have nearly equal influence on the slope and intercept of the line. However, the adjusted data used still introduce uncertainty of abscissa and ordinate values. Because of this as well as the possibility of rounding off errors, exchanging the monomer  $M_1$  and  $M_2$  will not give identical  $r_1$  and  $r_2$  values. It would seem appropriate to use the average so it would compensate the error. This will not rigorously justify statistical error but practically compensate it.

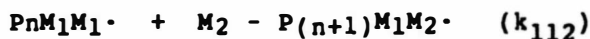
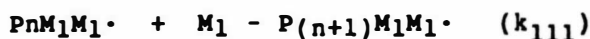
In the Intersection method as some intersection points have more uncertainty those points should be weighted much less heavily than the others to determine the average value. In calculations if the uncertainty of each value is weighted according to reciprocal square of the uncertainty, the intersection method becomes a very accurate method to calculate  $r_1$  and  $r_2$  values.

The experimental data in this research have led to another valuable observation. In Figure 5 for some of the concentrations

all the points either are above or below the calculated composition lines. This effect seen in Figure 11 gives a sinusoidal type wave instead of an expected straight line. As data points have a much better fit to a sinusoidal curve than to a horizontal straight line, this observation is probably not because of a random error in the copolymer composition studies. Normally this kind of error produces an irregular scattering of data points. This organized deviation from a straight line leads to the conclusion that there is a significant error in the assumed models, perhaps a penultimate unit effect.

Though such an effect was not expected to be found, it would be consistent with the existence of multiple chromophores in the UV spectra. Such chromophores imply a difference of electronic energy levels depending on neighboring units in the polymer. Such differences might also affect the reactivities of terminal units on the growing polymer radical, and thus the reactivity ratios might reasonably be affected by neighboring units.

In the penultimate unit model of copolymerization depending on the polar, steric and other characteristics of the reacting monomers, the next to the last monomer unit is thought to have an influence on the propagation reactions. If this is the case then eight propagation reactions are possible, which will lead to two  $r_1$  and two  $r_2$  values shown below.<sup>44-45</sup>



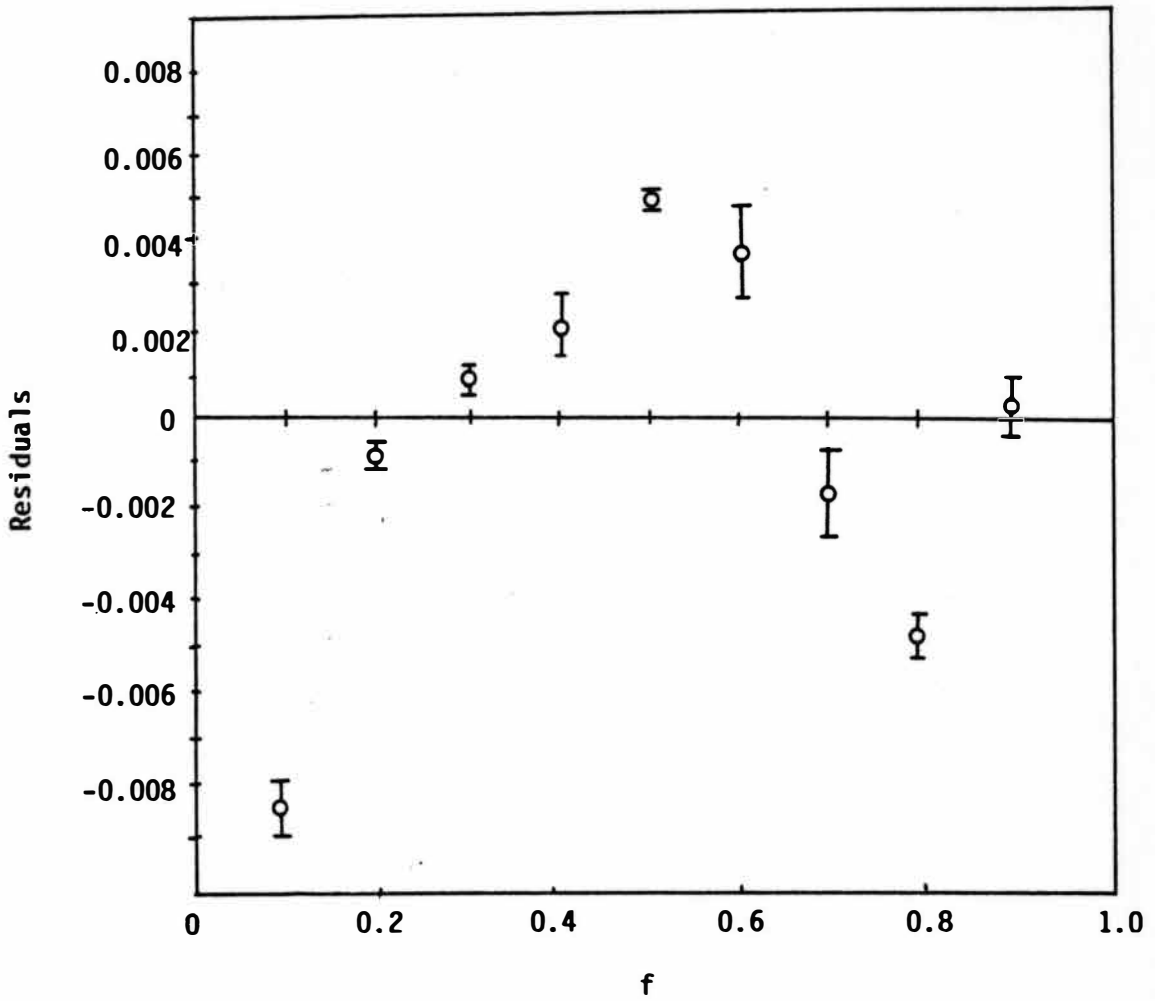


Figure 11. Analysis of Residuals from Non-Linear Least Squares Fitting. Lines represent 95% Confidence Limits.

$$P_n M_2 M_1 \cdot + M_1 - P_{(n+1)} M_1 M_1 \cdot \quad (k_{211})$$

$$P_n M_2 M_1 \cdot + M_2 - P_{(n+1)} M_1 M_2 \cdot \quad (k_{212})$$

$$P_n M_1 M_2 \cdot + M_1 - P_{(n+1)} M_2 M_1 \cdot \quad (k_{121})$$

$$P_n M_1 M_2 \cdot + M_2 - P_{(n+1)} M_2 M_2 \cdot \quad (k_{122})$$

$$P_n M_2 M_2 \cdot + M_1 - P_{(n+1)} M_2 M_1 \cdot \quad (k_{221})$$

$$P_n M_2 M_2 \cdot + M_2 - P_{(n+1)} M_2 M_2 \cdot \quad (k_{222})$$

$$r_1 = \frac{k_{111}}{k_{112}}$$

$$r_1' = \frac{k_{211}}{k_{212}}$$

$$r_2 = \frac{k_{222}}{k_{221}}$$

$$r_2' = \frac{k_{122}}{k_{121}}$$

#### Analysis of Ultraviolet Absorption Spectra of Styrene-Methyl Methacrylate Copolymer.

Although in this study refractive index increment measurements were used to determine the copolymer composition, some work has been done with the UV absorption analysis. These results are included with the hope of being of assistance in research that might be done in this area, as extensive studies of this subject were not found in the literature.

In UV analysis as explained in the Introduction chapter, a wavelength that is absorbed only by one monomer is chosen. It is



assumed that the other monomer has neither an absorption nor an indirect effect on the absorption of the chromophore unit.

Styrene was the chromophore selected in this copolymer, and it was assumed that absorption by methyl methacrylate units in the copolymer was negligible. However, there are some other factors that have to be considered. This aspect can easily be seen by the significant difference of the absorption versus concentration plots of pure polystyrene<sup>46</sup> and a copolymer of styrene in Figure 12. In the copolymer the relationship is linear until about thirty-five percent conversion but deviates from there on. The reason is thought to be that in polystyrene there are many adjacent benzene rings which will affect the electronic spectrum relative to a copolymer with isolated benzene rings.

This effect was observed in Figure 13 by overlapping the UV absorption spectrum of the various monomer feed compositions of styrene-methyl methacrylate copolymers containing the same concentration of styrene. The specific absorbance of each chromophore unit will differ depending on other chromophore units in the vicinity. This leads to three different situations when monomer sequence triads are considered. In previous studies<sup>7</sup> only diads were considered but in this study the use of triads was felt to be a better choice. These triads can be designated type I, II, and III, which refer to (BAB), (BAA or AAB) and (AAA) monomer sequences, respectively. In this case, styrene is the chromophore unit A and B is the methyl methacrylate unit. The relative concentrations

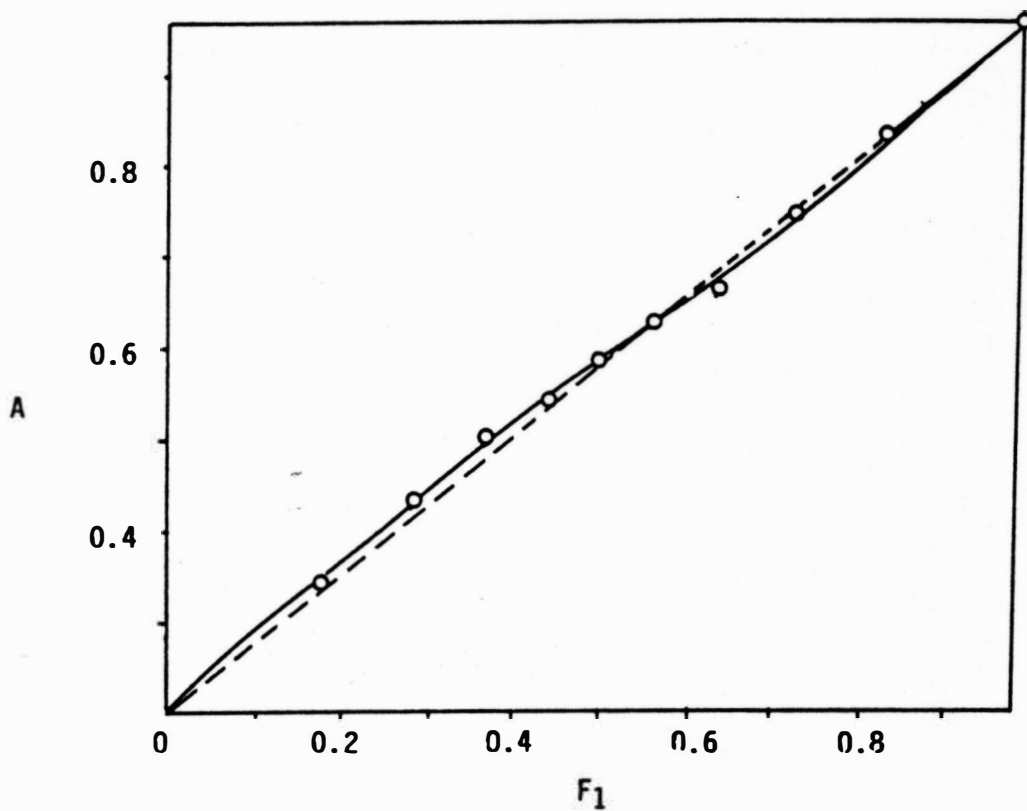


Figure 12. UV Absorbances of Styrene-Methyl Methacrylate Copolymer. Solid Line Represents Non-Linear Least Squares Fitted Curves Assuming Three Chromophores of Styrene Units. Dashed Line Represents Simple Beer's Law Curve.

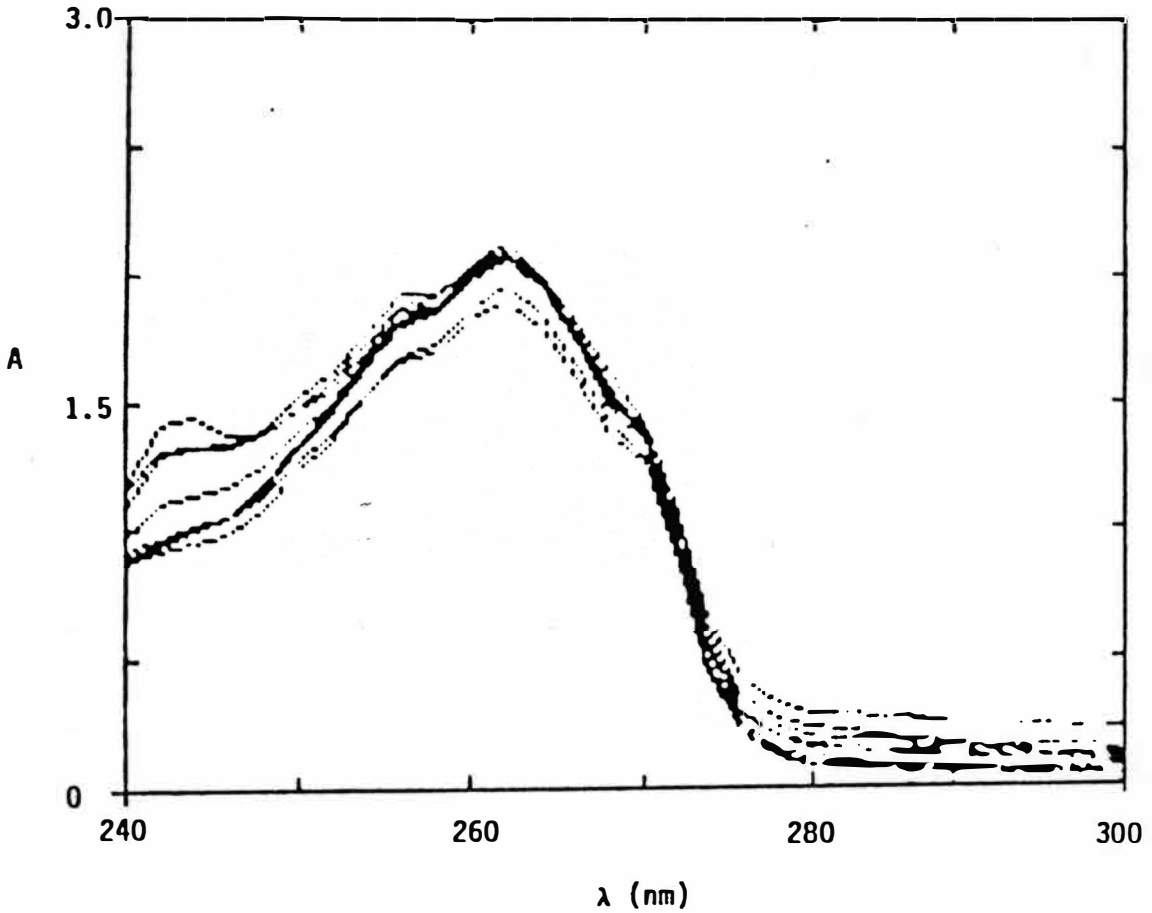


Figure 13. Overlapped Ultraviolet Absorption of the Various Monomer Feed Compositions of Styrene-Methyl Methacrylate Copolymers All Containing 1.0mg/mL of Styrene.

of the three types of units were computed using the overall best fit values of monomer reactivity ratios,  $r_1$  and  $r_2$ , in the following formulas,

$$\text{Fraction type I} = (1 - p_{11})K$$

$$\text{Fraction type II} = 2 p_{11}K$$

$$\text{Fraction type III} = \frac{p_{11}^2}{1 - p_{11}} K$$

where,  $p_{11}$  is the probability that a growing radical chain  $M_1\cdot$  will add to monomer  $M_1$ , and

$$p_{11} = \frac{r_1[M_1]}{r_1[M_1] + [M_2]}$$

Then,

$$(1 - p_{11})K + 2p_{11}K + \frac{p_{11}^2}{1 - p_{11}} K = 1$$

and  $K = 1 - p_{11}$

$K$  is the normalizing factor, so

$$\text{Fraction type I} = (1 - p_{11})^2$$

$$\text{Fraction type II} = 2p_{11}(1 - p_{11})$$

$$\text{Fraction type III} = p_{11}^2$$

Using values of  $r_1 = 0.49520$  and  $r_2 = 0.46669$ , a plot of the fraction of each type of triads versus mole percent styrene in monomer feed can be seen in Figure 14.

Finally the non-linear least square fitted values of the single wavelength UV absorbances of copolymers were plotted against concentration. Comparison with the observed absorbance values of the styrene-methyl methacrylate copolymer was made. These values are seen in Table 4 and the plot in Figure 12.

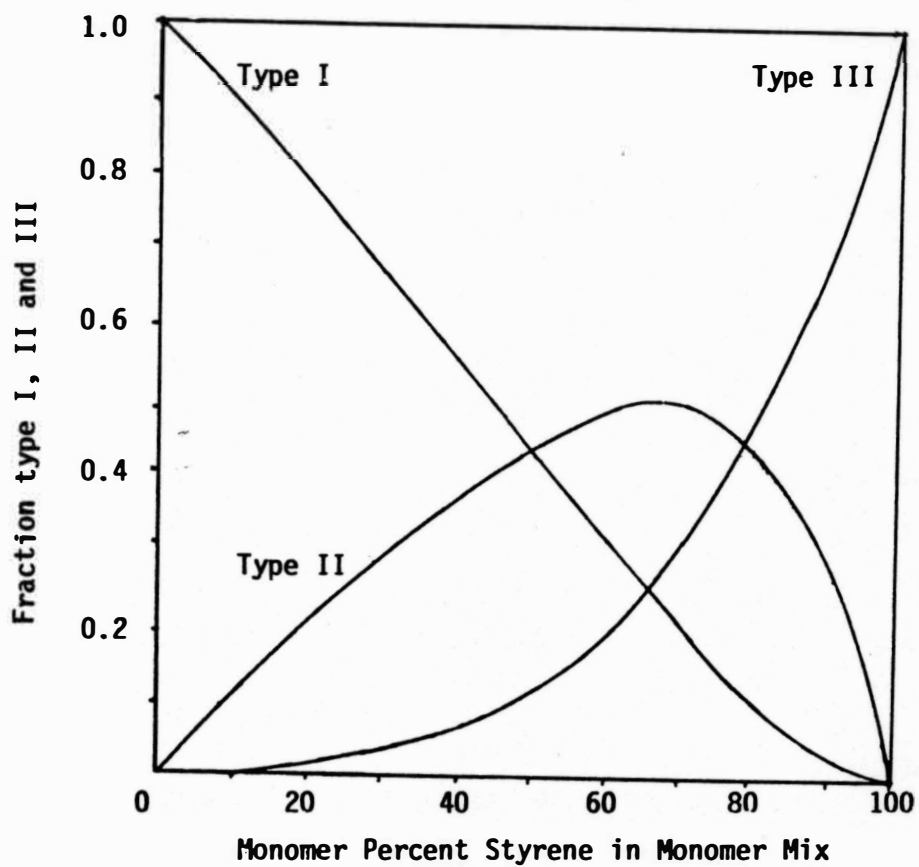


Figure 14. A Theoretical Plot of Triad Compositions as a Function of Monomer Compositions when  $r_1=0.495$  and  $r_2=0.467$ .

Table 4

## Experimental Values of Styrene-Methyl Methacrylate Copolymers

f	F <sub>1</sub>	A (observed)	A (calculated)	Residual	Specific Absorbance
0.099820	0.175574	0.282	0.2915	0.009504	1.6603
0.099820	0.175055	0.282	0.2906	0.008642	1.6603
0.200116	0.281153	0.462	0.4576	-0.004394	1.6276
0.200116	0.282241	0.462	0.4594	-0.002623	1.6276
0.300045	0.367232	0.601	0.5857	-0.015261	1.5950
0.300045	0.367106	0.601	0.5855	-0.015462	1.5950
0.400024	0.439254	0.683	0.6866	0.003613	1.5631
0.400024	0.439890	0.683	0.6876	0.004607	1.5631
0.499996	0.499916	0.769	0.7665	-0.002531	1.5332
0.499996	0.500376	0.769	0.7672	-0.001825	1.5332
0.600024	0.563827	0.850	0.8497	-0.000279	1.5071
0.600024	0.563119	0.850	0.8487	-0.001346	1.5071
0.699999	0.640948	0.923	0.9535	0.030538	1.4877
0.699999	0.640998	0.923	0.9536	0.030613	1.4877
0.799999	0.730519	1.092	1.0810	-0.010972	1.4798
0.799999	0.730305	1.092	1.0807	-0.011289	1.4798
0.899994	0.836827	1.265	1.2478	-0.017254	1.4910
0.899994	0.836298	1.265	1.2470	-0.018043	1.4910
1.000000	1.000000	1.518	1.5342	0.016200	1.5342

The specific absorbances shown in Table 4 are the effective specific absorbances of the composite of styrene units, normalized to unit styrene concentration rather than to unit polymer concentration in the solution being measured.

## Conclusions

The following conclusions can be derived from the results that were obtained in this study.

The composition of polymer changed with conversion as expected for the range of conversion study.

The rate of copolymerization when plotted against monomer composition gave essentially a J-shaped curve.

The maximum likelihood method is the best method to find the  $r_1$  and  $r_2$  values. The second best is the Non-Linear Least Squares method. The Intersection method ranks third, Kelen-Túdós fourth and Fineman-Ross fifth in accuracy. However, Kelen-Túdós appears to be a good method for routine determinations because of its simplicity and accuracy.

The effect of ignoring conversion in the calculations leads to significant errors in the reactivity ratios, even if the actual conversion is only a few percent.

In the UV region there appear to be several different chromophores in this copolymer, so that a simple application of Beer's Law is not valid for determining the composition.

## Recommendations

In this study all calculations were done assuming the absence of penultimate unit effects. However the analysis of residuals from statistical data fitting showed a strong possibility of a penultimate effect. Therefore, it is recommended that this factor be considered in further studies to obtain a better fit of experimental data to the theoretical data.

Another area of consideration is in the method of finding copolymer compositions with the aid of UV absorbances. In this study monomer sequence triads were used instead of diads which had been used in previous studies. Still it was assumed that methyl methacrylate monomer had no absorption at the wavelength selected. However, it is possible that methyl methacrylate has an absorption even though it probably is very small. Calculations including methyl methacrylate as a chromophore might therefore give more accurate copolymer composition values.

One other interesting research would be to do this study with monomers that have a much bigger difference in  $r_1$  and  $r_2$  values. This would result in a much larger composition drift. A comparison of methods to find  $r_1$  and  $r_2$  with such a copolymer system would increase the applicability of the results obtained in this research.



**APPENDICES**

**APPENDIX A**

**Experimental Data for Copolymerization of  
Styrene with Methyl Methacrylate**

**TABLE I**  
**Copolymerization at 60.0°C**

Sample Number	Mass of Monomer, g		Time polymerized, h	Copolymer formed, g
	Styrene	Methyl Methacrylate		
1	—	10.0928	1	0.5882
2	0.9977	8.6495	1	0.1769
3	1.0000	8.6388	2	0.4684
4	1.0070	8.6492	3	0.5817
5	1.0031	8.6468	4	0.8460
6	1.0023	8.6458	5	0.8934
7	1.0011	8.6600	6	1.2233
8	1.0008	8.6460	7	1.3431
9	1.0027	8.6563	8	1.5638
10	1.0008	8.6456	9	1.7207
11	2.0013	7.6906	1	0.1669
12	2.0029	7.7047	2	0.2669
13	2.0017	7.6867	2	0.4016
14	2.0027	7.6908	3	0.4369
15	2.0007	7.6874	3	0.4482
16	2.0027	7.6881	4	0.6575
17	2.0019	7.7009	5	0.8238
18	2.0012	7.6864	6	0.9553
19	2.0025	7.6937	7	1.0720
20	1.9966	7.6757	8	1.3983
21	1.9995	7.6905	9	1.4576
22	3.0008	6.7295	1	0.1096
23	3.0003	6.7291	1	0.1176
24	3.0004	6.7293	2	0.2971

TABLE I--Continued

Sample Number	Mass of Monomer, g		Time polymerized, h	Copolymer formed, g
	Styrene	Methyl Methacrylate		
26	3.0007	6.7295	4	0.5921
27	2.9997	6.7287	4	0.6406
28	3.0007	6.7287	5	0.7407
29	2.9999	6.7286	6	0.9931
30	3.0008	6.7297	7	1.0844
31	3.0009	6.7296	8	1.3802
32		6.7295	9	1.6215
33		5.7674	1	0.1264
34		5.7679	2	0.2495
35		5.7680	3	0.3732
36		5.7680	4	0.6832
37		5.7681	4	0.4920
38		5.7678	5	0.7435
39		5.7682	5	0.5865
40		5.7680	6	0.7090
41		5.7681	7	0.7573
42		5.7683	7	1.0579
43		5.7679	7	1.0852
44		5.7682	8	1.0250
45		5.7679	9	1.3714
46		5.7677	9	1.3040
47		4.8066	1	0.1217
48		4.8067	2	0.2492
49		4.8067	2	0.2095

TABLE I--Continued

Sample Number	Mass of Monomer, g		Time polymerized, h	Copolymer formed, g
	Styrene	Methyl Methacrylate		
51	4.9999	4.8063	4	0.5095
52	5.0002	4.8067	4	0.4504
53	5.0004	4.8069	5	0.5684
54	5.0002	4.8067	6	0.6646
55	5.0001	4.8069	7	0.7709
56	5.0004	4.8067	8	0.8747
57	5.0000	4.8066	9	0.9697
58	6.0004	3.8451	1	0.1481
59	6.0001	3.8449	1	0.0933
60	6.0000	3.8447	2	0.2029
61	6.0012	3.8454	2	0.1928
62	6.0009	3.8454	3	0.3692
63	6.0011	3.8455	3	0.3042
64	6.0010	3.8451	4	0.4823
65	6.0014	3.8454	4	0.4946
66	6.0008	3.8453	5	0.5959
67	6.0013	3.8455	5	0.5465
68	6.0007	3.8454	6	0.6199
69	6.0012	3.8456	7	0.7837
70	6.0013	3.8455	8	0.8281
71	6.0014	3.8456	9	0.8946
72	6.0008	3.8454	9	1.1034
73	7.0009	2.8843	1	0.1052
74	7.0013	2.8848	2	0.2002

TABLE I--Continued

Sample Number	Mass of Monomer, g		Time polymerized, h	Copolymer formed, g
	Styrene	Methyl Methacrylate		
76	7.0005	2.8843	4	0.4188
77	7.0012	2.8847	4	0.4197
78	7.0006	2.8843	5	0.4988
79	7.0002	2.8841	6	0.6184
80	7.0008	2.8844	7	0.7252
81	7.0004	2.8845	8	0.7951
82	7.0003	2.8840	9	1.0773
83	8.0003	1.9227	1	0.1103
84	8.0007	1.9230	1	0.0957
85	8.0010	1.9231	2	0.2084
86	8.0013	1.9235	2	0.2068
87	8.0009	1.9227	3	0.3320
88	8.0003	1.9225	3	0.3355
89	8.0010	1.9228	4	0.4014
90	8.0007	1.9229	4	0.3947
91	8.0011	1.9230	5	0.5249
92	8.0006	1.9229	5	0.5210
93	8.0011	1.9228	6	0.5937
94	8.0005	1.9229	7	0.6407
95	8.0004	1.9228	7	0.7794
96	8.0009	1.9230	8	0.7451
97	8.0007	1.9229	8	0.7474
98	8.0002	1.9228	9	0.9223
99	8.9998	0.9612	1	0.1104
100	9.0001	0.9613	1	0.0917

TABLE I--Continued

Sample Number	Mass of Monomer, g		Time polymerized, h	Copolymer formed, g
	Styrene	Methyl Methacrylate		
101	9.0003	0.9614	1	0.0950
102	9.0005	0.9615	2	0.2425
103	9.0010	0.9616	2	0.1940
104	9.0006	0.9614	3	0.3159
105	9.0002	0.9612	4	0.4207
106	9.0003	0.9613	4	0.4716
107	9.0002	0.9614	5	0.5972
108	9.0008	0.9615	5	0.5960
109	9.0001	0.9614	5	0.5527
110	9.0010	0.9617	6	0.6967
111	9.0004	0.9614	7	0.8119
112	9.0003	0.9615	7	0.8129
113	9.0009	0.9616	8	0.8443
114	9.0004	0.9615	8	0.9035
115	9.0011	0.9617	9	1.0616
116	10.1281	—	1	0.1439

**TABLE II**  
**Differential Refractive Index Increments**

Sample Number	$\frac{dn}{dc}$ in Methyl Ethyl Ketone	$\frac{dn}{dc}$ in Ethyl Acetate
1	0.1200	0.1177
2	0.1385	0.1362
3	0.1384	0.1361
4	0.1383	0.1360
5	0.1384	0.1360
6	0.1383	0.1359
7	0.1383	0.1358
8	0.1382	0.1357
9	0.1382	0.1356
10	0.1380	0.1355
11	0.1495	0.1474
12	0.1495	0.1473
13	0.1494	0.1473
14	0.1494	0.1472
15	0.1493	0.1473
16	0.1494	0.1472
17	0.1493	0.1471
18	0.1493	0.1471
19	0.1492	0.1470
20	0.1491	0.1468
21	0.1489	0.1467
22	0.1584	0.1562
23	0.1583	0.1561
24	0.1583	0.1560
25	0.1582	0.1561



TABLE II--Continued

Sample Number	$\frac{dn}{dc}$ in Methyl Ethyl Ketone	$\frac{dn}{dc}$ in Ethyl Acetate
26	0.1582	0.1560
27	0.1582	0.1559
28	0.1581	0.1559
29	0.1581	0.1558
30	0.1580	0.1557
31	0.1579	0.1556
32	0.1578	0.1555
33	0.1658	0.1637
34	0.1657	0.1636
35	0.1656	0.1635
36	0.1657	0.1635
37	0.1656	0.1634
38	0.1656	0.1634
39	0.1655	0.1633
40	0.1655	0.1633
41	0.1654	0.1631
42	0.1653	0.1630
43	0.1653	0.1630
44	0.1653	0.1630
45	0.1653	0.1629
46	0.1653	0.1629
47	0.1720	0.1699
48	0.1719	0.1699
49	0.1719	0.1699
50	0.1720	0.1699

TABLE II--Continued

Sample Number	$\frac{dn}{dc}$ in Methyl Ethyl Ketone	$\frac{dn}{dc}$ in Ethyl Acetate
51	0.1720	0.1699
52	0.1720	0.1699
53	0.1719	0.1699
54	0.1720	0.1698
55	0.1720	0.1699
56	0.1720	0.1699
57	0.1720	0.1698
58	0.1785	0.1763
59	0.1784	0.1765
60	0.1786	0.1766
61	0.1787	0.1767
62	0.1787	0.1766
63	0.1785	0.1768
64	0.1788	0.1769
65	0.1788	0.1769
66	0.1789	0.1770
67	0.1787	0.1769
68	0.1788	0.1771
69	0.1789	0.1772
70	0.1789	0.1773
71	0.1790	0.1773
72	0.1790	0.1773
73	0.1863	0.1842
74	0.1865	0.1843
75	0.1866	0.1844

TABLE II--Continued

Sample Number	$\frac{dn}{dc}$ in Methyl Ethyl Ketone	$\frac{dn}{dc}$ in Ethyl Acetate
76	0.1868	0.1845
77	0.1868	0.1845
78	0.1869	0.1845
79	0.1870	0.1846
80	0.1870	0.1847
81	0.1871	0.1848
82	0.1872	0.1849
83	0.1953	0.1932
84	0.1953	0.1932
85	0.1954	0.1933
86	0.1955	0.1934
87	0.1955	0.1934
88	0.1956	0.1935
89	0.1956	0.1935
90	0.1956	0.1935
91	0.1957	0.1936
92	0.1958	0.1937
93	0.1957	0.1937
94	0.1958	0.1937
95	0.1959	0.1938
96	0.1959	0.1938
97	0.1959	0.1938
98	0.1960	0.1939
99	0.2059	0.2038
100	0.2059	0.2038

TABLE II--Continued

Sample Number	$\frac{dn}{dc}$ in Methyl Ethyl Ketone	$\frac{dn}{dc}$ in Ethyl Acetate
101	0.2059	0.2038
102	0.2059	0.2039
103	0.2060	0.2039
104	0.2061	0.2040
105	0.2062	0.2040
106	0.2061	0.2041
107	0.2062	0.2041
108	0.2063	0.2042
109	0.2063	0.2042
110	0.2064	0.2043
111	0.2066	0.2044
112	0.2067	0.2044
113	0.2067	0.2044
114	0.2068	0.2045
115	0.2069	0.2046
116	0.2220	0.2200

**APPENDIX B**

**Calculated Values of Composition and Conversion  
for Copolymerization of Styrene  
with Methyl Methacrylate**

**TABLE I**  
**Conversion as a Function of Time**  
**of Polymerization at 60.0°C**

Sample Number	Percent Conversion by mass	Percent Conversion by mole	Time of Polymerization, h
1	1.4207	—	1
2	1.8367	1.8281	1
3	4.8595	4.8451	2
4	6.0241	6.0065	3
5	8.7671	8.7409	4
6	9.2600	9.2327	5
7	12.6621	12.6248	6
8	13.9228	13.8826	7
9	16.1901	16.1431	8
10	17.8377	17.7873	9
11	1.7221	1.7165	1
12	2.7494	2.7405	2
13	4.1452	4.1320	2
14	4.5071	4.4928	3
15	4.6263	4.6117	3
16	6.7848	6.7632	4
17	8.4903	8.4635	5
18	9.8611	9.8300	6
19	11.0559	11.0215	7
20	14.4567	14.4123	8
21	15.0423	14.9971	9
22	1.1264	1.1234	1
23	1.2087	1.2055	1
24	3.0535	3.0455	2
25	4.6763	4.6641	3

TABLE I--Continued

Sample Number	Percent Conversion by mass	Percent Conversion by mole	Time of Polymerization, h
26	6.0852	6.0694	4
27	6.5848	6.5678	4
28	7.6130	7.5936	5
29	10.2082	10.1821	6
30	11.1443	11.1163	7
31	14.1843	14.1492	8
32	16.6655	16.6249	9
33	1.2941	1.2921	1
34	2.5542	2.5503	2
35	3.8205	3.8149	3
36	6.9937	6.9831	4
37	5.0365	5.0291	4
38	7.6119	7.6007	5
39	6.0037	5.9951	5
40	7.2582	7.2477	6
41	7.7525	7.7417	7
42	10.8293	10.8145	7
43	11.1099	11.0947	7
44	10.4928	10.4785	8
45	14.0397	14.0206	9
46	13.3503	13.7616	9
47	1.2410	1.2410	1
48	2.5411	2.5412	2
49	2.1363	2.1364	2
50	3.6606	3.6606	3

TABLE I--Continued

Sample Number	Percent Conversion by mass	Percent Conversion by mole	Time of Polymerization, h
51	5.1957	5.1957	4
52	4.5927	4.5927	4
53	5.7957	5.7959	5
54	6.7769	6.7769	6
55	7.8607	7.8607	7
56	8.9190	8.9191	8
57	9.8882	9.8883	9
58	1.5042	1.5064	1
59	0.9477	0.9491	1
60	2.0610	2.0639	2
61	1.9580	1.9607	2
62	3.7496	3.0936	3
63	3.0894	3.7550	3
64	4.8984	4.9048	4
65	5.0229	5.0295	4
66	6.0521	6.0598	5
67	5.5500	5.5575	5
68	6.2959	6.3041	6
69	7.9589	7.9690	7
70	8.4098	8.4205	8
71	9.0850	9.0962	9
72	11.2064	11.2201	9
73	1.0642	1.0667	1
74	2.0251	2.0296	2
75	3.2362	3.2433	3



TABLE I--Continued

Sample Number	Percent Conversion by mass	Percent Conversion by mole	Time of Polymerization, h
76	4.2368	4.2458	4
77	4.2454	4.2544	4
78	5.0461	5.0566	5
79	6.2564	6.2692	6
80	7.3362	7.3512	7
81	8.0436	8.0597	8
82	10.8991	10.9205	9
83	1.1116	1.1419	1
84	0.9644	0.9670	1
85	2.0999	2.1056	2
86	2.0837	2.0892	2
87	3.3456	3.3544	3
88	3.3811	3.3899	3
89	4.0448	4.0553	4
90	3.9774	3.9877	4
91	5.2891	5.3027	5
92	5.2502	5.2638	5
93	5.9825	5.9978	6
94	6.4565	6.4727	7
95	7.8543	7.8738	7
96	7.5081	7.5268	8
97	7.5315	7.5502	8
98	9.2946	9.3173	9
99	1.1083	1.1110	1
100	0.9206	0.9228	1

TABLE I--Continued

Sample Number	Percent Conversion by mass	Percent Conversion by mole	Time of Polymerization, h
101	0.9537	0.9560	1
102	2.4343	2.4402	2
103	1.9473	1.9520	2
104	3.1710	3.1786	3
105	4.2233	4.2332	4
106	4.7341	4.7455	4
107	5.9950	6.0091	5
108	5.9826	5.9963	5
109	5.5484	5.5611	5
110	6.9931	7.0089	6
111	8.1501	8.1679	7
112	8.1602	8.1777	7
113	8.4748	8.4929	8
114	9.0696	9.0886	8
115	10.6556	10.6776	9
116	5.8279	—	1

TABLE II  
 Concentration of Styrene Units in the Monomer Feed and in  
 the Styrene-Methyl Methacrylate Copolymer

Sample Number	Styrene in Monomer		Styrene in Copolymer			
	mass fraction $x_1^o$	mole fraction $f_1^o$	From $dn/dc$ Measurements in Methyl Ethyl Ketone		From $dn/dc$ Measurements in Ethyl Acetate	
			mass fraction $X_1$	mole fraction $F_1$	mass fraction $x_1$	mole fraction $F_1$
1	0.0000	0.0000	—	—	—	—
2	0.1034	0.0998	0.1814	0.1756	0.1808	0.1751
3	0.1037	0.1001	0.1804	0.1746	0.1799	0.1741
4	0.1043	0.1007	0.1794	0.1737	0.1789	0.1731
5	0.1039	0.1003	0.1804	0.1746	0.1789	0.1731
6	0.1039	0.1003	0.1794	0.1737	0.1779	0.1722
7	0.1036	0.1000	0.1794	0.1737	0.1769	0.1712
8	0.1037	0.1001	0.1784	0.1727	0.1760	0.1703
9	0.1038	0.1002	0.1784	0.1727	0.1750	0.1693
10	0.1037	0.1001	0.1764	0.1708	0.1740	0.1684
11	0.2065	0.2001	0.2892	0.2812	0.2903	0.2822
12	0.2063	0.1999	0.2892	0.2812	0.2893	0.2813
13	0.2066	0.2002	0.2882	0.2802	0.2893	0.2813
14	0.2066	0.2002	0.2882	0.2802	0.2884	0.2803
15	0.2065	0.2001	0.2873	0.2792	0.2893	0.2813
16	0.2067	0.2003	0.2882	0.2802	0.2884	0.2803
17	0.2063	0.1999	0.2873	0.2792	0.2874	0.2794
18	0.2066	0.2002	0.2873	0.2792	0.2874	0.2794
19	0.2065	0.2001	0.2863	0.2783	0.2864	0.2784
20	0.2064	0.2000	0.2853	0.2773	0.2845	0.2765

TABLE II--Continued

Sample Number	Styrene in Monomer		Styrene in Copolymer			
	mass fraction $x_1^o$	mole fraction $f_1^o$	From dn/dc Measurements in Methyl Ethyl Ketone		From dn/dc Measurements in Ethyl Acetate	
			mass fraction $X_1$	mole fraction $F_1$	mass fraction $X_1$	mole fraction $F_1$
21	0.2063	0.1999	0.2833	0.2754	0.2835	0.2755
22	0.3084	0.3000	0.3765	0.3672	0.3763	0.3671
23	0.3084	0.3000	0.3755	0.3662	0.3754	0.3661
24	0.3084	0.3000	0.3755	0.3663	0.3744	0.3652
25	0.3084	0.3000	0.3745	0.3653	0.3754	0.3661
26	0.3084	0.3000	0.3745	0.3653	0.3744	0.3652
27	0.3083	0.2999	0.3745	0.3653	0.3734	0.3642
28	0.3084	0.3001	0.3735	0.3643	0.3734	0.3642
29	0.3084	0.3000	0.3735	0.3643	0.3724	0.3632
30	0.3084	0.3000	0.3725	0.3634	0.3715	0.3623
31	0.3084	0.3000	0.3716	0.3624	0.3705	0.3613
32	0.4095	0.4000	0.3706	0.3614	0.3695	0.3603
33	0.4095	0.4000	0.4490	0.4393	0.4497	0.4399
34	0.4095	0.4000	0.4480	0.4383	0.4487	0.4389
35	0.4095	0.4000	0.4471	0.4373	0.4477	0.4379
36	0.4095	0.4000	0.4480	0.4383	0.4477	0.4379
37	0.4095	0.4000	0.4471	0.4373	0.4467	0.4370
38	0.4095	0.4000	0.4471	0.4373	0.4467	0.4370
39	0.4095	0.4000	0.4461	0.4363	0.4457	0.4360
40	0.4095	0.4000	0.4461	0.4363	0.4457	0.4360

TABLE II--Continued

Sample Number	Styrene in Monomer		Styrene in Copolymer			
	mass fraction $x_1^o$	mole fraction $f_1^o$	From dn/dc Measurements in Methyl Ethyl Ketone		From dn/dc Measurements in Ethyl Acetate	
			mass fraction $X_1$	mole fraction $F_1$	mass fraction $X_1$	mole fraction $F_1$
41	0.4095	0.4000	0.4451	0.4354	0.4438	0.4341
42	0.4095	0.4000	0.4441	0.4344	0.4428	0.4331
43	0.4095	0.4000	0.4441	0.4344	0.4428	0.4331
44	0.4095	0.4000	0.4441	0.4344	0.4428	0.4331
45	0.4095	0.4000	0.4441	0.4344	0.4418	0.4321
46	0.5099	0.5000	0.4441	0.4344	0.4418	0.4321
47	0.5099	0.5000	0.5098	0.4999	0.5103	0.5004
48	0.5099	0.5000	0.5088	0.4989	0.5103	0.5004
49	0.5099	0.5000	0.5088	0.4989	0.5103	0.5004
50	0.5099	0.5000	0.5098	0.4999	0.5103	0.5004
51	0.5099	0.5000	0.5098	0.4999	0.5103	0.5004
52	0.5099	0.5000	0.5098	0.4999	0.5103	0.5004
53	0.5099	0.5000	0.5088	0.4989	0.5103	0.5004
54	0.5099	0.5000	0.5098	0.4999	0.5093	0.4994
55	0.5099	0.5000	0.5098	0.4999	0.5103	0.5004
56	0.5099	0.5000	0.5098	0.4999	0.5103	0.5004
57	0.5099	0.5000	0.5098	0.4999	0.5093	0.4994
58	0.6095	0.6000	0.5735	0.5638	0.5728	0.5631
59	0.6095	0.6000	0.5725	0.5628	0.5748	0.5651
60	0.6095	0.6000	0.5745	0.5648	0.5757	0.5661

TABLE II--Continued

Sample Number	Styrene in Monomer		Styrene in Copolymer			
	mass fraction $x_1^o$	mole fraction $f_1^o$	From $dn/dc$ Measurements in Methyl Ethyl Ketone		From $dn/dc$ Measurements in Ethyl Acetate	
			mass fraction $x_1$	mole fraction $F_1$	mass fraction $x_1$	mole fraction $F_1$
61	0.6095	0.6000	0.5755	0.5658	0.5757	0.5661
62	0.6095	0.6000	0.5755	0.5658	0.5757	0.5661
63	0.6095	0.6000	0.5735	0.5638	0.5777	0.5680
64	0.6095	0.6000	0.5765	0.5668	0.5787	0.5690
65	0.6095	0.6000	0.5765	0.5668	0.5787	0.5690
66	0.6095	0.6000	0.5774	0.5678	0.5797	0.5700
67	0.6095	0.6000	0.5755	0.5658	0.5787	0.5690
68	0.6095	0.6000	0.5765	0.5668	0.5806	0.5710
69	0.6095	0.6000	0.5774	0.5678	0.5816	0.5720
70	0.6095	0.6000	0.5774	0.5678	0.5826	0.5730
71	0.6095	0.6000	0.5784	0.5687	0.5826	0.5730
72	0.6095	0.6000	0.5784	0.5687	0.5826	0.5730
73	0.7082	0.7000	0.6500	0.6409	0.6500	0.6410
74	0.7082	0.7000	0.6520	0.6429	0.6510	0.6420
75	0.7082	0.7000	0.6530	0.6439	0.6520	0.6430
76	0.7082	0.7000	0.6550	0.6459	0.6530	0.6440
77	0.7082	0.7000	0.6550	0.6459	0.6530	0.6440
78	0.7082	0.7000	0.6560	0.6568	0.6530	0.6440
79	0.7082	0.7000	0.6570	0.6479	0.6540	0.6450
80	0.7082	0.7000	0.6570	0.6479	0.6549	0.6460

TABLE II--Continued

Sample Number	Styrene in Monomer		Styrene in Copolymer			
	mass fraction $x_1^o$	mole fraction $f_1^o$	From dn/dc Measurements in Methyl Ethyl Ketone		From dn/dc Measurements in Ethyl Acetate	
			mass fraction $x_1$	mole fraction $F_1$	mass fraction $x_1$	mole fraction $F_1$
81	0.7082	0.7000	0.6580	0.6489	0.6559	0.6470
82	0.7082	0.7000	0.6590	0.6499	0.6569	0.6480
83	0.8062	0.8000	0.7382	0.7305	0.7380	0.7303
84	0.8062	0.8000	0.7382	0.7305	0.7380	0.7303
85	0.8062	0.8000	0.7392	0.7315	0.7390	0.7313
86	0.8062	0.8000	0.7402	0.7325	0.7400	0.7323
87	0.8062	0.8000	0.7402	0.7325	0.7400	0.7323
88	0.8062	0.8000	0.7412	0.7335	0.7410	0.7333
89	0.8062	0.8000	0.7412	0.7335	0.7410	0.7333
90	0.8062	0.8000	0.7412	0.7335	0.7410	0.7333
91	0.8062	0.8000	0.7422	0.7345	0.7420	0.7343
92	0.8062	0.8000	0.7431	0.7355	0.7430	0.7353
93	0.8062	0.8000	0.7422	0.7345	0.7430	0.7353
94	0.8062	0.8000	0.7431	0.7355	0.7430	0.7353
95	0.8062	0.8000	0.7441	0.7365	0.7439	0.7363
96	0.8062	0.8000	0.7441	0.7365	0.7439	0.7363
97	0.8062	0.8000	0.7441	0.7365	0.7439	0.7363
98	0.8062	0.8000	0.7451	0.7375	0.7449	0.7373
99	0.9035	0.9000	0.8422	0.8368	0.8416	0.8363
100	0.9035	0.9000	0.8422	0.8368	0.8416	0.8363

TABLE II--Continued

Sample Number	Styrene in Monomer		Styrene in Copolymer			
	mass fraction $x_1^o$	mole fraction $f_1^o$	From $dn/dc$ Measurements in Methyl Ethyl Ketone		From $dn/dc$ Measurements in Ethyl Acetate	
			mass fraction $X_1$	mole fraction $F_1$	mass fraction $X_1$	mole fraction $F_1$
101	0.9035	0.9000	0.8422	0.8368	0.8416	0.8363
102	0.9035	0.9000	0.8422	0.8368	0.8426	0.8373
103	0.9035	0.9000	0.8431	0.8378	0.8426	0.8373
104	0.9035	0.9000	0.8441	0.8388	0.8436	0.8383
105	0.9035	0.9000	0.8451	0.8398	0.8436	0.8383
106	0.9035	0.9000	0.8441	0.8388	0.8446	0.8393
107	0.9035	0.9000	0.8451	0.8398	0.8446	0.8393
108	0.9035	0.9000	0.8461	0.8409	0.8456	0.8403
109	0.9035	0.9000	0.8461	0.8409	0.8456	0.8403
110	0.9035	0.9000	0.8471	0.8419	0.8465	0.8413
111	0.9035	0.9000	0.8490	0.8439	0.8475	0.8423
112	0.9035	0.9000	0.8500	0.8449	0.8475	0.8423
113	0.9035	0.9000	0.8500	0.8449	0.8475	0.8423
114	0.9035	0.9000	0.8510	0.8459	0.8485	0.8433
115	0.9035	0.9000	0.8520	0.8469	0.8495	0.8443
116	1.0000	1.0000	—	—	—	—



## REFERENCES

1. Billmeyer, F. W. "Textbook of Polymer Science", 2nd ed., New York: Interscience, 1971, Chapter 11.
2. Wall, F. T. The Structure of Vinyl Copolymers. J. Am. Chem. Soc., 1941, 63, 1862-1870.
3. Mayo, F. R., and Lewis, F. M. A Basis for Comparing the Behavior of Monomers in Copolymerization; The Copolymerization of Styrene and Methyl Methacrylate. J. Am. Chem. Soc., 1944, 66, 1594-1601.
4. Alfrey, T., and Goldfinger, G. The Mechanism of Copolymerization. J. Phys. Chem., 1944, 12, 205-210.
5. Critchfield, F. E., and Johnson, D. P. Chemical Analysis of Polymers. Anal. Chem., 1961, 33, 1834-1836.
6. Funt, B. L., and Collins, E. Formation of Block Polymers of Butyl Acrylate with Styrene and Vinyl Pyridine. J. Polym. Sci., 1958, 28, 359-364.
7. Tobolsky, A. V., Eisenberg, A., and O'Driscoll, K. F. Spectrophotometric Determination of Styrene in a Styrene-Methyl Methacrylate Copolymer. Anal. Chem., 1959, 31, 203-204.
8. O'Driscoll, K. F., Wertz, W., and Husar, A. Influence of Intra-chain Interactions on the Kinetics of Styrene Polymerization and Copolymerization. J. Polym. Sci., 1967, 5A, 2159-2166.
9. Brussau, R. J., and Stein, D. J. Abhängigkeit der UV-Absorption binärer Styrol-Copolymerisate von der Länge der Styrolsequenzen. Angew. Macromol. Chem., 1970, 12, 59-71.
10. Gallo, B. M., and Russo, S. Ultraviolet Absorption Spectra of Styrene Copolymers. I. Solvent Effects on the Hypochromism of Poly(Styrene-co-Methyl Methacrylate) at 2695 Å°. J. Macromol. Sci.-Chem., 1974, A8, 521-531.
11. Gallo, B. M., and Russo, S. Structure and Properties of Random, Alternating, and Block Copolymers: The UV Spectra of Styrene-Methyl Methacrylate Copolymers. Adv. Chem. Ser., 1975, 142, 85-91.
12. Stutzel, B., Miyamoto, T., and Cantow, H. J. Hypochromic Effects in UV Spectra of Polymers in Solution. Polym. J., 1976, 8, 247-253.
13. Gruber, E., and Knell, W. L. Bestimmung der Chemischen Heterogenität Statistischer Copolymerer anhand von Untersuchungen and Poly(Styrol-co-Butyl Acrylat) und Poly(Styrol-co-Butyl Methacrylat). Macromol. Chem., 1978, 179, 733-746.

14. Runyon, J. R., Barnes, D. E., Rudd, J. F., and Tung, L. H. Multiple Detectors for Molecular Weight and Composition Analysis of Copolymers by Gel Permeation Chromatography. J. Appl. Polym. Sci., 1969, 13, 2359-2369.
15. Johnson, M., Karmo, T. S., and Smith, R. R. High Conversion Copolymerization of Styrene with Methyl Methacrylate. Eur. Polym. J., 1978, 14, 409-414.
16. Dionisio, J. M., and O'Driscoll, K. F. High-Conversion Copolymerization of Styrene and Methyl Methacrylate. J. Polym. Sci., Polym. Lett. Ed., 1979, 17, 701-707.
17. Garcia-Rubio, L. H. The Effect of Composition, Sequence Length, and Tacticity on the UV Absorption Analysis of Styrene Copolymers in Solution. J. Appl. Polym. Sci., 1982, 27, 2043-2052.
18. Colthup, N. B., Daly, L. H., and Wiberly, S. E. "Introduction to Infrared and Raman Spectroscopy" New York: Academic Press, 1964, Chapter 13.
19. Bellamy, L. S. "The Infrared Spectra of Complex Molecules", London: Chapman and Hall Ltd., 1975, Chapter 5.
20. Dollish, F. R., and Fateley, W. G. "Characteristic Raman Frequencies of Organic Compound", New York: John Wiley and Sons, 1974, Chapter 6.
21. Angood, A. C., and Koenig, J. L. Effect of Nonrandom Polymer Chain Orientation in the Thickness Direction on Infrared Absorption Measurements. Macromolecules, 1969, 2, 37-42.
22. Bovey, F. A. "High Resolution NMR of Macromolecules", New York: Academic Press, 1972, Chapter 4.
23. Barrall, E. M., Contow, M. J. R., and Johnson, J. F. Variation of Refractive Index of Polystyrene with Molecular Weight: Effect on the Determination of Molecular Weight Distributions. J. Appl. Polym. Sci., 1968, 12, 1373-1377.
24. Francois, J., Candow, F., and Benoit, H. Effect of Molecular Weight on the Partial Specific Volume of Polystyrenes in Solution. Polymer, 1974, 15, 618-626.
25. Stockmayer, W. H., Moore, L. D., Fixman, M., and Epstein, B. N. Copolymers in Dilute Solution. I. Preliminary Results for Styrene-Methyl Methacrylate. J. Polym. Sci., 1955, 16, 517-530.
26. Bushuk, W., and Benoit, H. Light-scattering Studies of Copolymers. 1. Effect of Heterogeneity of Chain Composition on the Molecular Weight. Can. J. Chem., 1958, 36, 1616-1626.

27. Krause, S. Light Scattering of Copolymers. I. The Composition Distribution of a Styrene-Methyl Methacrylate Block Copolymer. J. Phys. Chem., 1961, 65, 1616-1623.
28. "Brice-Phoenix Visual Differential Refractometer Catalog" The Virtis Company, Inc., New York.
29. Ham, G. E. Reactivity of Polar Monomers in Copolymerization. J. Polym. Sci., 1954, 14, 87-93.
30. Fineman, M., and Ross, S. D. Linear Method for Determining Monomer Reactivity Ratios in Copolymerization. J. Polym. Sci., 1950, 5, 259-265.
31. Kelen, T., and Tüdös, F. Analysis of the Linear Methods for Determining Copolymerization Reactivity Ratios. I. A New Improved Linear Graphic Method. J. Macromol. Sci.-Chem., 1975, 179, 1-27.
32. Skeist, I. Copolymerization: The Composition Distribution Curve. J. Am. Chem. Soc., 1946, 68, 1781-1784.
33. Meyer, V. E., and Lowry, G. G. Integral and Differential Binary Copolymerization Equations. J. Polym. Sci., 1965, 3A, 2843-2851.
34. Kruse, R. L. The Simplified Calculation of Average Copolymer Composition Versus Extent of Polymeriation. J. Polym. Sci., Polymer Letters, 1967, 5, 437-440.
35. Lewis, F. M., Walling, C., Cumming, W., Briggs, E. R., and Mayo, F. R. Copolymerization. IV. Effects of Temperature and Solvents on Monomer Reactivity Ratios. J. Am. Chem. Soc., 1948, 70, 1519-1423.
36. Lewis, F. M., Mayo, F. R., and Hulse, W. F. Copolymerization, II. The Copolymerization of Acrylonitrile, Methyl Methacrylate, Styrene and Vinylidene Chloride. J. Am. Chem. Soc., 1945, 67, 1701-1705.
37. Wiley, R. H., and Sale, E. E. Tracer Techniques for the Determination of Monomer Reactivity Ratios. I. A Direct Counting Technique Applied to the Styrene-Methacrylate Copolymerization. J. Polym. Sci., 1960, 42, 479-489.
38. Price, C. C., and Walsh, J. G. Effect of Dielectric Solvent Medium on Copolymerization. J. Polym. Sci., 1951, 6, 239-242.
39. Meyer, V. E. Copolymerization of Styrene and Methyl Methacrylate Reactivity Ratios from Conversion-Composition Data. J. Polym. Sci. A.1., 1966, 4, 2819-2830.

40. Lewis, F. M., and Mayo, F. R. Precise Method for Isolation of High Polymers. J. Anal. Chem., 1945, 1, 134-136.
41. Timmermans, J. "Physico-Chemical Constants of Pure Organic Compounds." New York:Elsevier Publishing Co. 1950, 361, 415-416.
42. Lowry, G. G., and Kana'an, S. A. "Statistical Treatment of Experimental Errors in Physical Chemistry Laboratory Supliment" Western Michigan University.
43. Walling, C. Overall Rates in Copolymerization. Polar Effects in Chain Initiation and Termination. J. Am. Chem. Soc., 1949, 71, 1930-1935.
44. Ham, G. E. "Copolymerization" New York: Interscience, 1964, Chapter 1.
45. Merz, E., Alfrey, T., and Goldfinger, G. Intramolecular Reaction in Vinyl Polymers as a Means of Investigation of the Propagation Step. J. Polym. Sci., 1946, 1, 75-83.
46. Newel, J. E. Residual Monomer in Polystyrene. Anal. Chem., 1951, 23, 445-447.